Target-agnostic identification of human antibodies to Plasmodium falciparum sexual forms reveals cross stage recognition of glutamate-rich repeats

Axelle Amen, Randy Yoo, Amanda Fabra-García, Judith Bolscher, William J. R. Stone, Isabelle Bally, Sebastián Dergan-Dylon, Iga Kucharska, Roos de Jong, Marloes de Bruijni, et al.

eLife

Immunology and Inflammation
Microbiology and Infectious Disease

Reviewed Preprint
v2 • August 28, 2024
Revised by authors

Reviewed Preprint
v1 • May 23, 2024

Target-agnostic identification of human antibodies to *Plasmodium falciparum* sexual forms reveals cross stage recognition of glutamate-rich repeats

Axelle Amen, Randy Yoo, Amanda Fabra-García, Judith Bolscher, William JR Stone, Isabelle Bally, Sebastián Dergan-Dylon, Iga Kucharska, Roos M de Jong, Marloes de Bruijni, Teun Bousema, C Richter King, Randall S MacGill, Robert W Sauerwein, Jean-Philippe Julien, Pascal Poignard, Matthijs M Jore

CNRS, Univ. Grenoble Alpes, CEA, UMR5075, Institut de Biologie Structurale, Grenoble, France • CHU Grenoble Alpes, Grenoble, France • Program in Molecular Medicine, The Hospital for Sick Children Research Institute, Toronto, Canada • Department of Biochemistry, University of Toronto, Toronto, Canada • Department of Medical Microbiology, Radboudumc, Nijmegen, the Netherlands • TropIQ Health Sciences, Nijmegen, the Netherlands • Department of Immunology and Infection, London School of Hygiene and Tropical Medicine, London, United Kingdom • Center for Vaccine Innovation and Access, PATH, Washington, DC, USA • Department of Immunology, University of Toronto, Toronto, Canada • Department of Immunology and Microbiology, The Scripps Research Institute, La Jolla, USA

Abstract

Circulating sexual stages of *Plasmodium falciparum (Pf)* can be transmitted from humans to mosquitoes, thereby furthering the spread of malaria in the population. It is well established that antibodies (Abs) can efficiently block parasite transmission. In search for naturally acquired Ab targets on sexual stages, we established an efficient method for target-agnostic single B cell activation followed by high-throughput selection of human monoclonal antibodies (mAbs) reactive to sexual stages of *Pf* in the form of gamete and gametocyte extract. We isolated mAbs reactive against a range of *Pf* proteins including well-established targets Pfs48/45 and Pfs230. One mAb, B1E11K, was cross-reactive to various proteins containing glutamate-rich repetitive elements expressed at different stages of the parasite life cycle. A crystal structure of two B1E11K Fab domains in complex with its main antigen, RESA, expressed on asexual blood stages, showed binding of B1E11K to a repeating epitope motif in a head-to-head conformation engaging in affinity-matured homotypic interactions. Thus, this mode of recognition of *Pf* proteins, previously described only for PfCSP, extends to other repeats expressed across various stages. The findings augment our understanding of immune-pathogen interactions to repeating elements of the *Plasmodium* parasite proteome and underscore the potential of the novel mAb identification method used to provide new insights into the natural humoral immune response against *Pf*.

Impact Statement

A naturally acquired human monoclonal antibody recognizes proteins expressed at different stages of the *Plasmodium falciparum* lifecycle through affinity-matured homotypic interactions with glutamate-rich repeats

eLife assessment

This study reports **important** results and new insights into humoral immune responses to Plasmodium falciparum sexual stage proteins. The experiments are based on the use of target-agnostic memory B cell sorting and screening approaches as well as several state-of-the-art technologies. The authors present **compelling** evidence that one antibody, B1E11K, is cross-reactive with multiple proteins containing glutamate-rich repeats through homotypic interactions, a process similar to what has been observed for Plasmodium circumsporozoite protein repeat-directed antibodies.

https://doi.org/10.7554/eLife.97865.2.sa3

Introduction

The eradication of malaria remains a global health priority. In 2021, 247 million people were diagnosed with malaria with over 619,000 people succumbing to the disease (1). Malaria is caused by *Plasmodium* parasites: unicellular eukaryotic protozoans that transmit to human hosts through an *Anopheles* mosquito vector. Although insecticide-treated nets and various antimalarial compounds have aided in controlling the spread and combating severe clinical complications of the disease, mosquito and parasite strains resistant to such interventions have emerged (2). Thus, there is an urgent need to develop other technologies, such as vaccines, to help combat the spread of malaria, and eventually, contribute to the eradication of the disease.

The development of a highly efficacious malaria vaccine has been challenging, owing to the complex life cycle of malaria-causing parasites. The life cycle of *Plasmodium spp.* can be categorized into three distinct stages: the pre-erythrocytic, asexual blood stage, and sexual stages. Each step features the parasite undergoing large-scale morphological changes accompanied by modifications in proteomic expression profiles - with several proteins being exclusively expressed in a single stage (3). Therefore, vaccine-mediated humoral responses must be robust enough to generate sufficiently high-quality antibody responses to eliminate the majority of parasites at the stage the vaccine targets. As a result, one approach to vaccine development has focused on targeting “bottlenecks” in the parasite’s life cycle where the number of parasites is low (4) (5).

The pre-erythrocytic stage - following the transmission of sporozoites to humans by a bite from an infected mosquito - is a bottleneck targeted by the only two malaria vaccines recommended by the World Health Organization, RTS,S/AS01 and R21/Matrix-M (6) (7). The vaccines are based on the circumsporozoite protein (CSP) - an essential protein expressed at high density on the surface of the parasite during the pre-erythrocytic stage (8) (9) (10). In its central domain, the protein contains various four amino acid repeat motifs - the most predominant of those being NANP repeats. Protective antibodies elicited against CSP primarily target this immunodominant repeat region. A large proportion of these antibodies engage in homotypic interactions which are

characterized by direct interactions between two antibodies' variable regions when bound to adjacent repetitive epitopes (11) (12) (13) (14) (15) (16) (17) (18) (19). Such interactions have been demonstrated to augment B cell activation and contribute to shaping the humoral response to CSP (12). Although these first-generation malaria vaccines only induce short-lived efficacy in a subset of the at-risk population (20), they will undoubtedly assist in lowering the overall incidence of malaria in young infants with clear initial impact (21). Modeling suggests that for improvements towards eradication of the disease, combining multiple types of interventions that target different stages of the *Plasmodium* life cycle may strongly increase the efficacy of weaker interventions (22).

Another bottleneck in the parasite's life cycle occurs during its sexual stage, which takes place in the mosquito vector. This stage begins when intraerythrocytic *Plasmodium* gametocytes, which are capable of eliciting antibody responses through clearance in the spleen (23), are taken up through a mosquito bloodmeal. Once inside the mosquito midgut, gametocytes emerge from erythrocytes and mature into gametes which then undergo fertilization ultimately resulting in the generation of sporozoites that can go on to infect the next human host. Vaccines that aim to target this life cycle bottleneck are known as transmission-blocking vaccines (TBVs) (24). The goal of TBVs is to elicit antibodies that target sexual stage antigens to block the reproduction of the parasite in the mosquito and thus onward transmission to humans. Current TBV development efforts are primarily focused on two antigens, Pfs230 and Pfs48/45, as they are the targets of the most potent transmission-blocking antibodies identified to date (25) (26) (27) (28). Indeed, individuals with sera enriched in antibodies that target Pfs230 and Pfs48/45 were found to have high transmission-reducing activity (29). Protective responses to Pfs230 and Pfs48/45 are well characterized at a molecular and structural level (26) (27) (28) (30) (31) (32) (33) (34). However, sera depleted in antibodies targeting the pro domain and domain 1 of Pfs230 and domains 2 and 3 of Pfs48/45 can retain transmission-reducing activity while maintaining the ability to recognize the surface of parasites lacking Pfs48/45 and Pfs230 surface expression (29). This highlights the importance of expanding our understanding of antibody responses to other sexual stage antigens.

We designed a workflow for the isolation of Abs to sexual stage specific antigens from a donor who was repeatedly exposed to malaria parasites. Our efforts yielded a panel of 14 monoclonal antibodies (mAbs) targeting Pfs230 and Pfs48/45 as well as other unidentified proteins, some with transmission-reducing activity. One mAb exhibited cross-reactivity to multiple antigens present at various stages of the parasite's life cycle, by targeting glutamate-rich repeats and engaging in homotypic interactions. This latest result underscores a pivotal role of repetitive elements in shaping the humoral response to *Pf*.

Results

Agnostic memory B cell (MBC) sorting and activation identifies potential *Pf* sexual stage protein-specific mAbs

We selected donor A, a 69-year-old Dutch expatriate who resided in Central Africa for approximately 30 years and whose serum was shown to strongly reduce *Pf* transmission, to isolate sexual stage-specific mAbs. We previously demonstrated the serum of this donor, donor A, largely retained its transmission-reducing activity (TRA) when depleted of antibodies directed against the main transmission-blocking epitopes of Pfs48/45 and *Pf*s230 (29), suggesting the presence of antibodies targeting other epitopes on these 2 proteins or directed at other proteins also involved in transmission.

PBMCs from the donor were thawed and a total of 1496 IgG+ memory B cells were sorted in 384-well plates (**Fig. 1**) (Fig. S1A). After activation, single cell culture supernatants potentially containing secreted IgGs were screened in a high-throughput 384-well ELISA for their reactivity against a crude *Pf* gamete lysate (Fig. S1B). A subset of supernatants was also screened against gametocyte lysate (S1C). In total, supernatants from 84 wells reacted with gamete and/or gametocyte lysate proteins, representing 5.6% of the total memory B cells. Of the 21 supernatants that were screened against both gamete and gametocyte lysates, six recognized both, while nine appeared to recognize exclusively gamete proteins, and six exclusively gametocyte proteins.

To isolate the corresponding mAbs, single B cell lysates from the 84 ELISA-positive wells were subjected to single B cell reverse transcriptase PCR (RT-PCR) for amplification of immunoglobulin variable genes. We obtained and cloned heavy and light chain sequences for 11 out of 84 wells. For three wells we obtained a kappa light chain sequence and for five wells a lambda light chain sequence. For three wells we obtained both a lambda and kappa light chain sequence suggesting that either both chains were present in a single B cell or that two B cells were present in the well. For all 14 wells we retrieved a single heavy chain sequence. Following amplification and cloning, 14 mAbs were expressed as full human IgG1s (Table S1) (Dataset S1). (34)

Isolated mAbs exhibit distinct patterns of recognition of gamete surface proteins

The 14 mAbs were first tested for binding to *Pf* sexual stage surface antigens in a surface immune-fluorescence assay using wild-type female gametes (**Fig. 2A**). The mAbs were also tested for binding to Pfs48/45 knock-out female gametes, which lack surface-bound Pfs48/45 and Pfs230 (35) (29) Seven mAbs exhibited binding to approximatively half or more of gametes when tested at a concentration of 100 µg/ml. Among these, four mAbs, B1C5K, B1C5L, B2C10L and B2E9L, recognized wild-type gametes with high scores (>68%) even at concentrations as low as 1 µg/ml. The binding of the B1C5K, B1C5L, B2C10L and B2E9L mAbs strongly decreased when using gametes that lacked surface-expressed Pfs48/45 and Pfs230, indicating that these four mAbs likely targeted one of these two antigens. Three other mAbs, B2D10L, B1C8L and B1E7K, displayed a similar recognition profile, albeit with notably smaller percentages of labeled wild-type gametes, particularly at the lower concentrations tested. This suggested a potential low affinity recognition of either Pfs48/45 or Pfs230 for these latter three mAbs.

Six of the remaining seven mAbs, B1C8K, B1D3L, B1D3K, B1F9K, B1C3L, and B2F7L, exhibited very weak or no binding to gametes. For B1C8K, this showed that the light chain (kappa) did not correspond to the antibody that was originally selected in the screening process as the lambda version (B1C8L) exhibited strong binding. As for the other mAbs, the results indicated that they may be specific for proteins not expressed or only poorly expressed at the gamete surface.

Finally, one mAb, B1E11K, exhibited a distinctive gamete surface binding profile, recognizing only a fraction (approximately a third to a fifth) of the wild-type and Pfs48/45 knock-out gametes across all tested concentrations, suggesting potential binding to non-Pfs48/45 and Pfs230 proteins.

Isolated mAbs have varying transmission-reducing activities and recognize different *Pf* sexual stage proteins

We were interested in investigating potential TRA for all identified mAbs. To do this, a standard membrane feeding assay (SMFA) was conducted in the presence of the isolated mAbs, revealing a range of transmission-reducing activities (**Fig. 2B**)(Table S2). Overall, seven mAbs were confirmed to strongly reduce transmission (TRA > 80%) when tested at 500 µg/ml: B1C5K, B1C5L, B2C10L, B2E9L, B1C8L, B1D3L and B1F9K. Of those, two mAbs, B1C8L and B2C10L retained >50% TRA at a lower concentration (100 µg/ml). Notably, despite not showing gamete surface

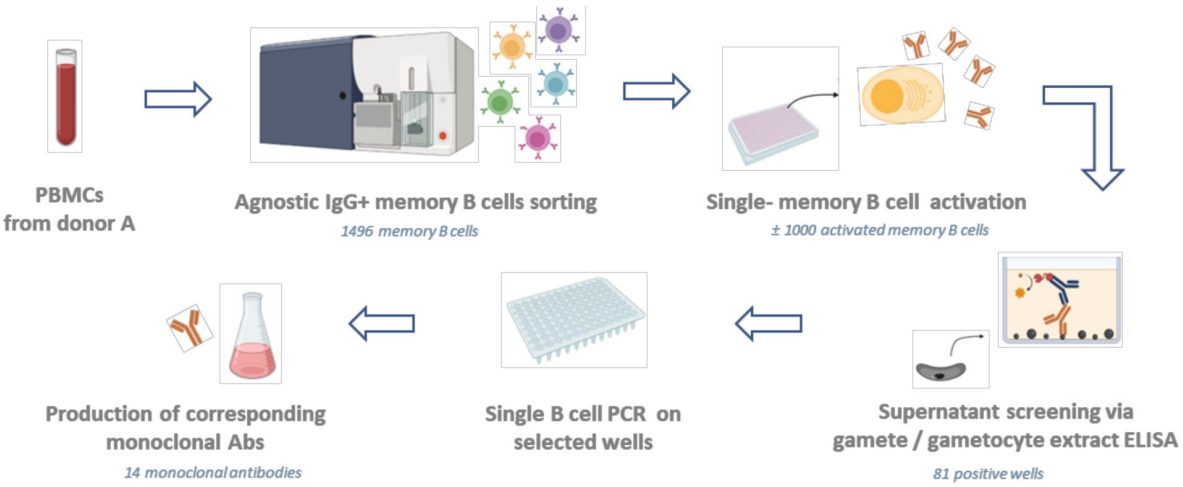

Figure 1

General workflow.

IgG+ memory B cells from Donor A were sorted individually regardless of their specificity, at one cell per well. Cells were further cultured in activation medium with CD40L-expressing feeder cells and cytokines to induce antibody secretion. Supernatants were tested for antibody binding to the sexual stage of the parasite through screening using a gamete extract ELISA. Memory B cells from wells displaying reactivity were selected for Ig genes amplification, followed by cloning and production of the corresponding antibody. Figure was created with Biorender.

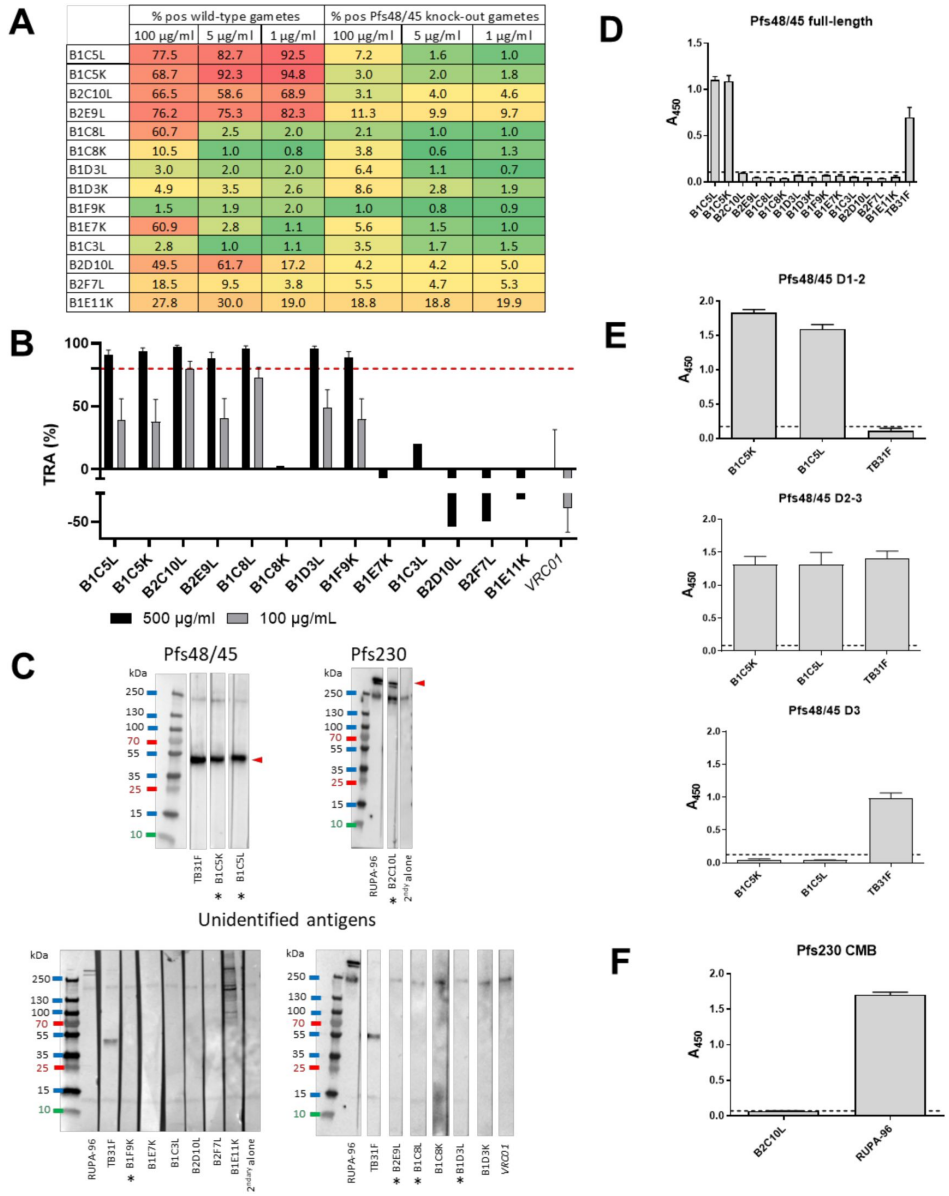

Figure 2

Characterization of the panel of isolated monoclonal antibodies.

(A) Percentage positive wild-type gametes and Pfs48/45 knock-out (KO) gametes that also lack surface bound Pfs230 in surface immunofluorescence assay, in a heatmap format (graded color scale: red for high percentage of binding, green for low percentage of binding). The experiment was performed in duplicate and three different monoclonal antibody concentrations were tested (100 µg/ml, 5 µg/ml and 1µg/ml). (B) Transmission reducing activity (TRA) of the mAb panel in standard membrane feeding assay (SMFA). For mAbs with >80% TRA at 500 µg/ml, experiments were run in duplicates and bars are estimates of the mean and error bars represent the 95% confidence intervals. mAbs with >80% TRA at 500 µg/ml were also tested at 100 µg/ml. Oocyst count data of the SMFA experiments can be found in Table S2. (C) Reactivity of the monoclonal antibody panel against gametocyte extract in Western blot, in non-reducing conditions. Antibodies are classified depending on the antigen recognized: Pfs48/45, Pfs230, or no antigen identified. TB31F is an anti-Pfs48/45 monoclonal antibody, RUPA-96 is an anti-Pfs230 monoclonal antibody, and VRC01 is an anti-HIV monoclonal antibody (negative control). Pfs48/45 and Pfs230 bands are indicated with a red arrow Antibodies with >80% TRA at 500 µg/ml are indicated with an asterisk (*). (D) Reactivity of the monoclonal antibody panel against full-length Pfs48/45 at 30 µg/ml in ELISA. (E) B1C5K and B1C5L binding to various Pfs48/45 domains in ELISA, at 10 µg/ml. (F) B2C10L binding to Pfs230 CMB domain in ELISA, at 10 µg/ml.

recognition, B1F9K and B1D3L displayed TRA - although only at high concentrations. Conversely, three mAbs recognizing the gamete surface, B2D10L, B1E7K and B1E11K, showed no activity in SMFA.

To gain deeper insight into the specificity of the various isolated mAbs, regardless of their transmission-reducing activity, we conducted further characterization via Western blot analyses using gametocyte extracts (**Fig. 2C**). The B1C5K and B1C5L mAbs recognized a protein with a molecular weight matching that of Pfs48/45. This result was consistent with the findings from the gamete surface binding experiment in which these mAbs recognized wildtype gametes but not Pfs48/45 knockout gametes, providing further validation of the specificity of the B1C5K and B1C5L mAbs in targeting Pfs48/45. The B2C10L mAb displayed pattern of recognition that corresponded to Pfs230, similar to the anti-Pfs230 control mAb RUPA-96 (26). Once again, these results were in agreement with the findings from the gamete surface binding experiment confirming the specificity of the B2C10L mAb in targeting Pfs230. The B1E11K mAb also appeared to bind to Pfs230 on the Western blot. However, in contrast to the RUPA-96 mAb, B1E11K only recognized the higher molecular band corresponding to Pfs230, suggesting exclusive recognition of the unprocessed form of this protein (36). Interestingly, besides Pfs230, B1E11K also recognized several unidentified proteins ranging from 70 and 250 kDa with various intensities. These findings were consistent with the gamete binding assay that showed recognition of gametes lacking Pfs48/45 and Pfs230, suggesting potential recognition of proteins other than Pfs48/45 and Pfs230. Finally, all the other mAbs showed no clear binding to any protein from the gametocyte extract on the Western blot. In the case of those demonstrating binding to gamete surfaces, B2E9L, B2D10L, B1C8L, B1E7K, this may be attributed to their recognition of conformational epitopes that are lost during Western blotting preparation, or possibly of specific recognition of proteins expressed in gametes but not gametocytes.

The recognition of Pfs48/45 by the B1C5K and B1C5L mAbs was subsequently confirmed through an ELISA using full-length recombinant Pfs48/45 (**Fig. 2D**). Notably, none of the other mAbs of the panel displayed binding to this Pfs48/45 recombinant protein construct. To further pinpoint the domain targeted by B1C5K and B1C5L, an ELISA was performed using constructs corresponding to domains 1-2, 2-3 and 3 revealing that these two mAbs targeted Domain 2 of Pfs48/45 (**Fig. 2E**). This is in agreement with prior work indicating mAbs to Domain 2 of Pfs48/45 are generally mAbs with low potency (27).

The combined findings above strongly pointed to Pfs230 as the target of mAb B2C10L. We thus tested this mAb in ELISA for binding to Pfs230CMB, a construct containing Pfs230 domain 1 and part of the pro-domain (37) No reactivity was observed (**Fig. 2F**) suggesting that B2C10L may recognize other Pfs230 domains than the one tested, or recognize epitopes not properly displayed in the construct used.

In summary, our target-agnostic mAb isolation approach successfully identified mAbs against *Pf* sexual stage proteins, some of which exhibited TRA and some of which target Pfs48/45 or Pfs230. However, given that the mAbs isolated in this study showed substantially lower TRA than mAbs identified previously (38) (39) we elected not to investigate them further. Instead, we were intrigued by the binding properties of B1E11K, which showed cross-reactivity with various *Pf* proteins, including Pfs230. Such cross-reactivity has been shown as a hallmark of the human Ab response to *Pf* and explored at the serum level but to our knowledge has never been studied at the mAb level (40) (41). Thus, we rationalized a more detailed molecular characterization of this mAb may provide insights into this relatively unexplored phenomenon.

The B1E11K mAb cross-reacts to distinct sexual and asexual stage *Pf* proteins containing glutamate-rich repeats

First, to ensure the ability of B1E11K to recognize different proteins in Western blotting experiments was not due to polyreactivity, the mAb was tested in ELISA against a panel of human proteins, single-stranded DNA (ssDNA) and lipopolysaccharide (LPS). The 4E10 mAb, a well-known anti-HIV gp41 polyreactive mAb (42), was used as a positive control. The B1E11K mAb did not bind any of the antigens on the panel at any significant level, even at a high 50 µg/ml concentration, and therefore polyreactivity was ruled out (Fig. S2A).

To identify antigens recognized by B1E11K, immunoprecipitation experiments were conducted using gametocyte extract. Proteins of different molecular weights were specifically detected in the B1E11K immunoprecipitate but not when using the anti-HIV control mAb (Fig. S2B). Mass spectrometry analysis of the corresponding gel slices revealed recognition of Pfs230, confirming the Western blot results.

The specificity of B1E11K was further tested using a protein microarray featuring recombinant proteins corresponding to putative antigens expressed at the sexual stage as well as proteins expressed at different stages of the *Pf* life cycle (29). The results showed that B1E11K exhibited high level reactivity (>8-fold higher than the negative control, minimum signal intensity rank 15th of 943 array targets) against several antigens, some expressed at the sexual stage (*i.e.* Pf11.1), others at the asexual stage (*i.e.* LSA3, RESA, RESA3) (**Fig. 3A**). Analysis of the primary amino acid sequence of the antigens recognized in the array suggested homology in several cases, based on the presence of glutamate-rich regions (Fig. S3). To analyze the numerous repeated motifs contained in these proteins, we used the RADAR (Rapid Automatic Detection and Alignment of Repeats) software (43). Although B1E11K recognition of Pfs230 fragments on the array was lower than our cut off for further analysis (3.4-fold higher than the negative control, maximum signal intensity rank 30th of 943 array targets), its sequence was also analyzed using RADAR due to its recognition by B1E11K in the immunoprecipitation experiments (Fig. S4). The analysis showed Pfs230 and several of the proteins recognized by B1E11K on the array contained diverse patterns of glutamate-rich repeats of different lengths and compositions. Among these proteins, Pfs230, Pf11.1, RESA, RESA3 and LSA3 presented the most similar glutamate repeats, following an “EE-XX-EE” pattern (Fig. S4). Pfs230 contains adjacent EE-VG-EE repeats which are located in the domain of the protein which is cleaved upon gametocyte egress from erythrocytes (44). RESA and RESA3 contain 20 and nine EE-NV-EE overlapping repeats at the C terminus of the protein, respectively. LSA3 contains two overlapping EE-NV-EE repeats. Finally, 221 non-adjacent EE-LV-EE repeats span the whole Pf11.1 megadalton protein.

To verify the recognition of the aforementioned proteins, a Western blot was performed with recombinant forms of RESA, RESA3, LSA3, and of a Pf11.1 domain (45) (**Fig. 3B**). Domain 1 of Pfs230, which does not contain the EE-VG-EE repeats, was also included. The results confirmed the binding of B1E11K to all the proteins tested except for Pfs230D1, as expected. Overall, the data showed that the B1E11K mAb recognizes various *Pf* proteins from different stages, all containing glutamate-rich repeats.

To validate the B1E11K mAb specifically targets glutamate-rich repeats, we synthesized five biotinylated peptides derived from the various repeats found in the proteins identified above to test for binding in sandwich ELISA experiments (**Fig. 3C**). Overall, the B1E11K mAb bound to all peptides (**Fig. 3D**). However, it exhibited a higher specificity for the RESA-derived peptides with an EC_{50} at least 100 times greater compared to EC_{50} values obtained with the other glutamate-rich peptides. Altogether, this suggests the main antigenic targets of B1E11K are RESA and RESA3, which contain the EENV repeats.

A

Peptide ID	Corresponding protein	Peptide position in the protein *Peptide length*	Normalised score	Corrected score
PF3D7_0220000	Liver Stage Antigen 3	67 to 822 *756*	6.253495	59988.5
PF3D7_0309100	OMD protein	Full length *187*	6.188559	57356
PF3D7_1149200	ring infected erythrocyte surface antigen 3 (RESA3)	65 to 587 *523*	6.193454	54235.5
PF3D7_0102200	ring infected erythrocyte surface antigen (RESA)	568 to 1085 (end) *518*	6.044558	53268
PF3D7_1127500	Protein disulfide isomerase	Full length *433*	5.913398	44843.5
PF3D7_1036300	Duffy binding like merozoite surface protein 2	423 to 762 *340*	5.433248	32032.5
PF3D7_0411700	conserved plasmodium protein	138	5.111879	25673.5
PF3D7_1038400	Pf 11.1	2980 to 3637 *658*	4.763914	21787
PF3D7_1149200	ring infected erythrocyte surface antigen 3	570 to 1090 *521*	4.723332	20946.5
PF3D7_0804500	uncharacterized protein	215	4.610963	19703
PF3D7_1038400	Pf 11.1	8737 to 9663 (end) *827*	3.986108	12776.5
PF3D7_1038400	Pf 11.1	7795 to 8628 *778*	3.757038	11117.5
PF3D7_0909000	uncharacterized protein	528	3.689088	10267
PF3D7_1038400	Pf 11.1	103 to 1024 *922*	3.242688	7017
PF3D7_0522400	uncharacterized protein	934	3.164308	6643.5

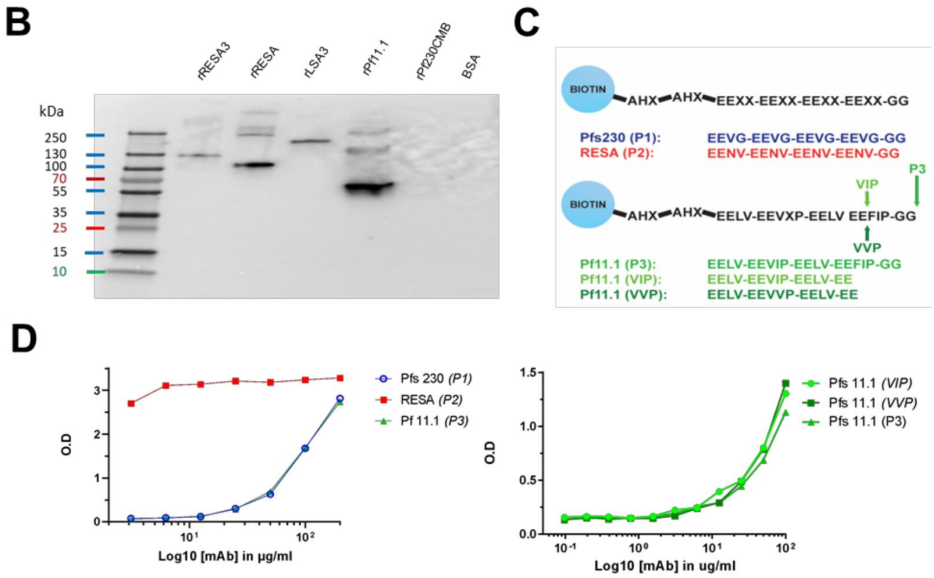

Figure 3

B1E11K binds repeat peptides.

(A) B1E11K binding to recombinant fragments of Pf proteins displayed on a microarray. (B) B1E11K binding to several recombinant proteins in Western blot, in non-reducing conditions. (C) Sequences of the peptides tested for binding. Peptides were N-terminally linked to a biotin moiety using aminohexanoyl (Ahx) spacers. (D) B1E11K binding in ELISA to a panel of peptides.

Since B1E11K bound to RESA-based peptides the strongest, we synthesized shorter RESA peptides for a more precise determination of the B1E11K minimal sequence epitope (**Fig. 4A**). When tested on the RESA peptide panel, B1E11K mAb binding to RESA P2 (16AA) and RESA 14AA, 12AA, and 10AA was similar, all exhibiting close EC_{50} values (**Fig. 4B**) (Fig. S6). No binding was observed for the 8AA RESA peptide, suggesting the 10AA peptide contained the minimal epitope. We hypothesized the similar EC_{50} values may be a result of avidity effects and thus, we performed the same experiment with recombinant B1E11K Fab (**Fig. 4C**). Although B1E11K Fab bound both RESA P2 (16AA) and RESA 14AA peptides with comparable strength of binding, both RESA 12AA and RESA 10AA peptides displayed comparatively poorer EC_{50} values with the RESA 10AA peptide displaying the lowest detectable binding strength. The binding affinity and kinetics of the interaction was also determined through biolayer interferometry (BLI). We performed experiments using the minimal sequence required for binding determined through ELISA [RESA 10AA peptide and the RESA P2 peptide (16AA)]. When immobilizing the peptide to the sensors, an approximately six-fold difference in affinity between the 10AA peptide (K_D = 484 nM) (**Fig. 4D**) and the P2 peptide (16AA) (K_D = 74 nM) (**Fig. 4E**) was observed.

Four EENV repeats permit two B1E11K Fabs to bind

Given the repetitive nature of the antigenic targets of B1E11K and differences in binding events captured in our BLI experiments, we hypothesized that more than one B1E11K Fab could potentially bind to the longer, RESA P2 (16AA) peptide. Thus, we performed isothermal titration calorimetry using the same two RESA peptides as in the BLI experiments to determine the binding stoichiometries. We observed when titrating the B1E11K Fab into RESA 10AA, a binding stoichiometry of N = 1.0 ± 0.2 (**Fig. 4F**) (**Table 1**). When using the RESA P2 (16AA) peptide, a stoichiometry of N = 2.1 ± 0.1 was observed (**Fig. 4G**) (**Table 1**). The determined binding affinity from our ITC experiments (**Table 1**) differed from our BLI experiments (**Fig. 4D** and **4E**), which can occur when measuring antibody-peptide interactions (46). Regardless, our data all trend toward the same finding in which a stronger binding affinity is observed toward the longer RESA P2 (16AA) peptide.

To further corroborate our binding stoichiometry findings, we performed size-exclusion chromatography coupled with multi-angle light scattering (SEC-MALS) to determine the molecular weight of the 2:1 Fab:peptide complex (**Fig. 4H**). We incubated a molar excess Fab:peptide (6:1) sample to saturate all B1E11K Fab binding sites present on the RESA peptide to obtain a solution containing the putative complex and excess monomeric Fab. The resulting chromatogram revealed two species eluted from the column. The molecular weight of the heavier species was in line with what would be expected from a 2:1 Fab:peptide complex (92 kDa) in which the mass determined fell within the range of experimental error. A negative-stain electron microscopy (nsEM) map reconstruction of the 2:1 Fab:peptide complex recovered from the SEC-MALS experiment (**Fig. 4H**) permitted the fitting of two Fab molecules, further supporting the 2:1 binding model (**Fig. 4I**).

B1E11K binds EENV repeats in a head-to-head conformation leveraging homotypic interactions

To obtain a full structural understanding of the observed repeat cross-reactivity and selectivity for RESA exhibited by B1E11K, we solved a 2.6 Å crystal structure of the B1E11K:RESA P2 (16AA) peptide complex (**Fig. 5A**) (**Table 2**) (Dataset 2). The electron density at the binding interface is unambiguous and included density for the entirety of the repeat region of the peptide (Fig. S6). Looking at the binding interface between the two Fabs and peptide reveals the structural basis for cross-reactivity (**Table 1**) (Fig. S7) (Table S3). The paratope of B1E11K is highly enriched in arginine and histidine residues giving rise to a highly electropositive groove (**Fig. 5B**-**5D**). These residues form a plethora of salt-bridging interactions with the glutamate residue side chains of RESA repeats (**Fig. 5E**). These interactions are supplemented by hydrogen bonding

Figure 4

Binding Characteristics of RESA peptides to B1E11K.

(A) Various peptides based on the EENV repeat region were designed and conjugated to a biotin-AHX-AHX moiety (AHX = ε-aminocaproic acid). EC_{50} values obtained from ELISA experiments utilizing various EENV repeat peptides with (B) B1E11K mAb or (C) B1E11K Fab. Error bars represent standard deviation. Biolayer interferometry experiments utilizing immobilized (D) RESA 10AA peptide or (E) RESA P2 (16AA) peptide dipped into B1E11K Fab. Representative isothermal titration calorimetry experiments in which B1E11K Fab was injected into (F) RESA 10AA peptide or (G) RESA P2 (16AA) peptide. (H) Size-exclusion chromatography coupled with multi-angle light scattering (SEC-MALS) of a solution of B1E11K Fab incubated with RESA P2 (16AA) peptide in a 6:1 molar ratio. The predicted molecular weight of the B1E11K Fab and RESA P2 peptide are 46.9 kDa and 2.5 kDa respectively. The shaded region indicates the fractions collected used for negative stain electron microscopy. (I) A nsEM map reconstruction which permits the fitting of two B1E11K Fabs (Fab A and Fab B).

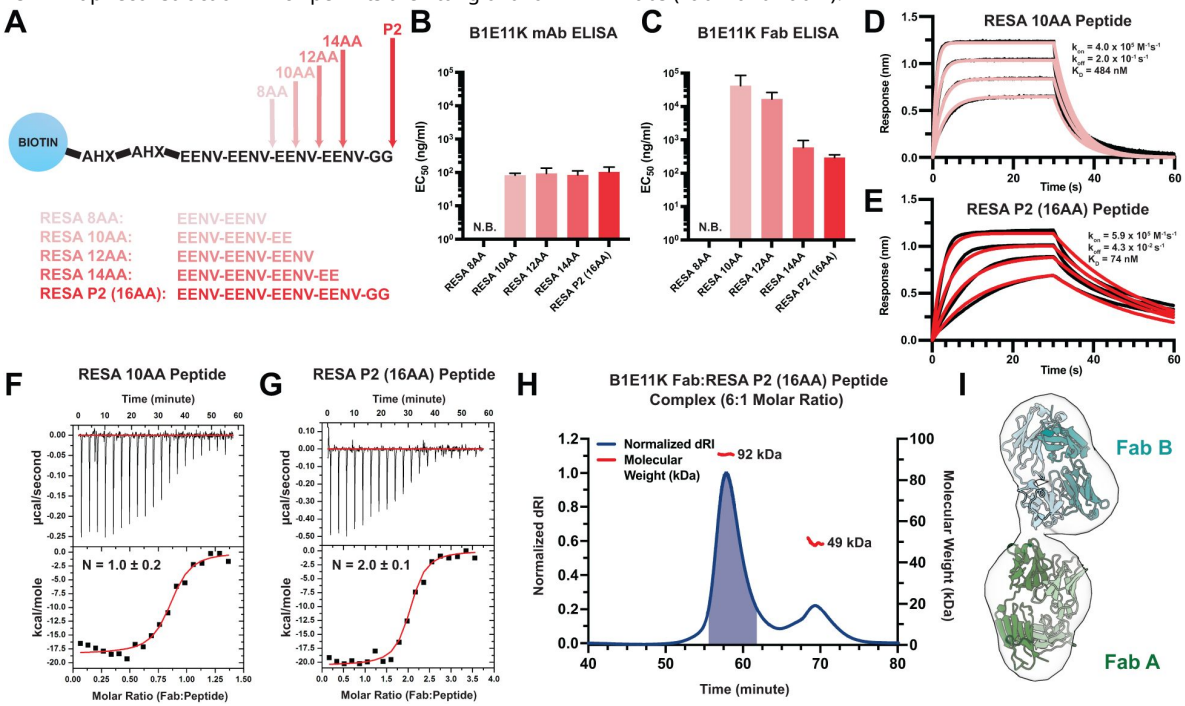

Table 1

ITC thermodynamics and binding affinity of B1E11K Fab to RESA peptides.

	RESA 10AA peptide (n=2)	RESA P2 peptide (n=3)
N	1.0 ± 0.2	2.1 ± 0.1
K_D (nM)	78 ± 12	73 ± 21
ΔG (kcal/mole)	-9.7 ± 0.3	-9.8 ± 0.3
ΔH (kcal/mole)	-18.3 ± 0.1	-20.5 ± 0.1
-TΔS (kcal/mole)	8.6 ± 0.2	10.7 ± 0.3

Error reported as standard deviation.

interactions of backbone serine and glycine residues of the B1E11K paratope as well as a hydrogen bond involving W33 found in the heavy chain of Fab B. Multiple hydrogen bonding interactions are made with B1E11K through the side chains of the asparagine residues of RESA repeats (EENV) (**Fig. 5F**) that would not exist in the context of binding to the repeats of Pf11.1 (EELV or EEVIP or EEFIP or EEVVP) or Pfs230 (EEVG) (**Fig. 3C**), as these residues lack side chains that can form hydrogen bonds. This likely leads to the observed higher specificity of B1E11K for RESA repeats demonstrated in our ELISA experiments (**Fig. 3D**).

Additionally, the crystal structure of the antibody-antigen complex revealed the presence of homotypic antibody-antibody contacts, through two interfaces surrounding the repeat peptide binding groove (**Fig. 5G**) (Fig. S8) (Table S4). The first interface features a salt-bridging network involving D60 of the Fab B kappa chain forming two salt bridges with R52 and H52A of the Fab A HCDR2 (**Fig. 5H**). Additionally, R54 of the Fab A HCDR2 forms two hydrogen bonds and a salt bridge with the Fab B kappa chain side chains of S55 and E56. Finally, Y58 of the Fab B HCDR2 forms a hydrogen bond with the side chain of S53 of the Fab A HCDR2. The second interface is less extensive featuring two hydrogen bonds between Y32 and S31 of the Fab B HCDR1 and the Fab A KCDR1 T29 and R27, respectively (**Fig. 5I**).

Analysis of the B1E11K sequences with IgBLAST (47) reveals that the B1E11K heavy and light chain have high similarity to the IGHV3-7 and IGKV3-20 germline sequences (Fig. S8). This analysis also indicates multiple residues involved in the homotypic interaction interface have undergone somatic hypermutation. Residues of the CDR2 heavy chain of Fab A, R52 and H52A, and kappa chain CDR1 residues of Fab B, T29 and R27, form various electrostatic and van der Waals interactions which are mutated from the inferred germline sequences (**Fig. 5F** and **5G**) (Fig. S8-9). In summary, our biophysical and structural characterization revealed the basis of cross-reactivity and specificity to RESA repeats (EENV) through a binding interface highly electrostatic in nature, featuring affinity-matured homotypic interactions between adjacent antibody molecules when in its antigen-bound state.

Discussion

Here, we introduce an innovative strategy that circumvents the use of recombinant proteins, to explore humoral immunity to *Pf* sexual proteins. We used target-agnostic MBC sorting and activation, followed by screening to assess reactivity against *P. falciparum* gamete lysate and, for a fraction of the sorted cells, gametocyte lysate. The approach enabled the identification of a panel of mAbs targeting diverse *Pf* proteins, including some that exhibit transmission reducing activity. The total number of isolated Abs was relatively low due to the limited number of cells used. However, the identified B cells accounted for 5.6% of the total number, which suggest that there is a relatively high proportion of B cells specific for gamete proteins in the memory compartment of this donor, considering not all B cells were activated (typically 70-80 % activation in our experiments). Furthermore, despite screening with a parasite extract containing a mixture of intracellular and surface proteins, half of the mAbs displayed binding to the surface of gametes, and/or exhibited TRA. This suggests antibody responses to surface proteins and proteins involved in transmission were high in this particular donor, potentially explaining the potent TRA observed with the serum.

Among the seven mAbs exhibiting TRA, three were found to recognize the well-defined TRA targets Pfs48/45 and Pfs230. The B1C5L and B1C5K mAbs were shown to recognize Domain 2 of Pfs48/45 and exhibited moderate potency, as previously described for antibodies with such specificity (27). These 2 mAbs were isolated from the same well and shared the same heavy chain; their similar characteristics thus suggest that their binding is primarily mediated by the heavy chain. Furthermore, a mAb identical to B1C5K was recently isolated from the same donor using a single B cell selection approach with recombinant Pfs48/45 (27). The B2C10L mAb was

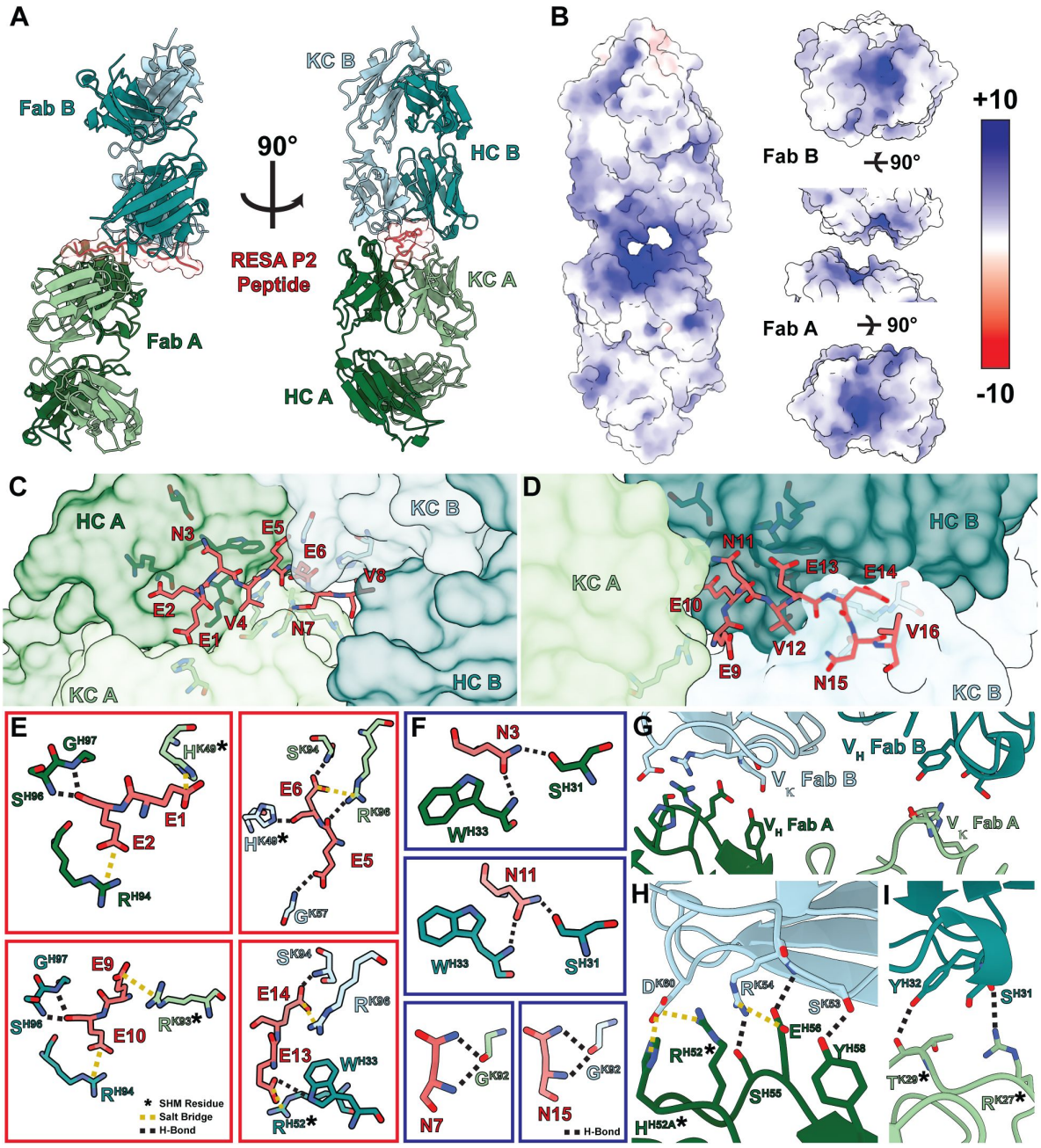

Figure 5

Structure of the B1E11K Fab and RESA P2 (16AA) peptide complex.

(A) The overall architecture of the B1E11K:RESA P2 (16AA) peptide complex. (B) The electrostatic potential of the surface of the B1E11K Fabs. Fab residues involved in electrostatic interactions with (C) residues 1-8 and (D) 9-16 of the RESA P2 peptide are shown as sticks. (E) Electrostatic interactions occurring with glutamate residues of the RESA P2 (16AA) peptide. Residues that have undergone somatic hypermutation (SHM) are marked with an asterisk. Salt bridges are shown as dashed yellow lines and hydrogen bonds as dashed black lines. (F) Hydrogen bonding interactions through the asparagine residues of the RESA P2 (16AA) peptide are shown as black dashed lines. (G) Variable heavy (V_H) and variable kappa (Vκ) residues involved in homotypic interactions are shown as sticks. (H) The first interaction interface and (I) second interface. Residues that have undergone somatic hypermutation (SHM) are marked with an asterisk. Electrostatic interactions are presented as dashed lines and coloured as done previously.

Crystal	B1E11K:RESA P2 (16AA) peptide
Beamline	APS-23-ID-B
Wavelength (Å)	1.0332
Space group	C 2 2 2_1
Cell dimensions	
a,b,c (Å)	78.7, 186.3, 131.5
α, β, γ (°)	90, 90, 90
Resolution (Å)[a]	40.0 - 2.53 (2.65 – 2.56)
No. molecules in ASU	1
No. of observations	236,070 (23,834)
No. unique observations	31,520 (3,067)
Multiplicity	7.5 (7.8)
R_{merge} (%)[b]	14.5 (222.8)
R_{pim} (%)[c]	5.7 (85.5)
<I/σI>	10.8 (1.0)
$CC_{1/2}$ (%)	99.7 (36.5)
Completeness (%)	99.8 (98.5)
Refinement Statistics	
Reflections used in refinement	31,512
Reflections used in R-free	1,575
Non-hydrogen atoms	6,781
Macromolecule	6,627
Water	130
Heteroatom	24
R_{work}[d] / R_{free}[e] (%)	21.5 / 24.5
Rms deviations from ideality	
Bond lengths (Å)	0.002
Bond angle (°)	0.48
Ramachandran plot	
Favoured regions (%)	96.0
Allowed regions (%)	3.8
Ramachandran outliers (%)	0.2
B-factors (Å^2)	
Wilson B-factor	65.5
Average B-factors	89.8
Average macromolecule	90.3
Average Heteroatom	83.1
Average water molecule	61.0

[a]Values in parentheses refer to the highest resolution bin.
[b]$R_{merge} = \Sigma_{hkl} \Sigma_i | I_{hkl,\,i} - \langle I_{hkl} \rangle | / \Sigma_{hkl} \langle I_{hkl} \rangle$
[c]$R_{pim} = \Sigma_{hkl} [1/(N-1)]^{1/2} \Sigma i | I_{hkl,\,i} - \langle I_{hkl} \rangle | / \Sigma_{hkl} \langle I_{hkl} \rangle$
[d]$R_{work} = (\Sigma | |Fo| - |Fc| |) / (\Sigma | |F_o|)$ - for all data except as indicated in footnote e.
[e]5% of data were used for the R_{free} calculation.

Table 2

Crystallography statistics.

shown to recognize Pfs230 in gamete binding assays and western blot, but failed to bind the pro and D1 domains of Pfs230 in ELISA. This confirms TRA may be mediated through binding to domains other than pro-D1, the current main vaccine candidate (48), as previously observed for rodent mAbs that were generated against native Pfs230 (49) (50) (51).

The remaining four mAbs exhibiting TRA did not clearly demonstrate recognition of either Pfs230 or Pfs48/45. Among those mAbs, B2E9L, and to a lesser extent B1C8L, showed recognition of wildtype gametes but not gametes that lacked surface-bound Pfs230 and Pfs48/45. However, Western blot did not identify any protein targeted by these two mAbs and they did not bind to Pfs48/45 in ELISA. Therefore, we hypothesize these two mAbs target a protein associated with the Pfs48/45-Pfs230 complex (52). An alternative explanation for the antigenicity of B2E9L and B1C8L is that these two mAbs may target a Pfs230 conformational epitope that is not represented in Western blot assays. The last two mAbs that exhibited TRA, B1D3L and B1F9K, displayed no reactivity with the gamete surface, neither with wildtype nor gametes that lacked surface-bound Pfs48/45 and Pfs230, and did not show any recognition in Western blot. In the case of B1D3L, the selection during screening was based on recognition of the gametocyte lysate while testing on the gamete extract was negative. This mAb may possibly target a protein only expressed on gametocytes (indicating that the epitope might be conformational and not properly displayed in Western blotting with gametocyte extract). Regarding B1F9K, it is somewhat surprising that this mAb, which was originally selected based on positivity in the gamete extract ELISA, did not display reactivity in SIFA while still exhibiting TRA. Further exploration is needed to understand this apparent discrepancy. Overall, these latter mAbs, which do not recognize well-defined TRA targets, demonstrated lower potency in the SMFA assay compared to some of the best characterized mAbs with such activity. Nevertheless, they could still be of strong interest in defining potential novel TRA targets, and further investigations are needed.

Seven of the fourteen mAbs isolated did not exhibit TRA. Of those, four exhibited some level of binding to gamete surfaces: B1E11K, B2D10L, B1E7K and B2F7L (albeit very weakly). This may suggest either the recognition of proteins involved in transmission but with an insufficient affinity to exert a significant effect, recognition of non-functional epitopes in proteins that play a role in transmission, or the recognition of proteins unrelated to the transmission process altogether.

B1E11K recognized various proteins from both the Pf sexual stage and asexual stages, all containing glutamate-rich repeats. Repetitive regions rich in glutamate residues have been previously found to be highly immunogenic in malaria-experienced individuals. A study investigating antibody responses against asexual stage antigens of *Pf* associated with erythrocyte invasion using sera from individuals from various cohorts found that the repetitive regions rich in glutamate residues within these antigens were predominantly recognized (40). Another investigation into sera from individuals from Uganda corroborated this finding (41). Raghavan et al noted the antibodies that target these repeats may be potentially cross-reactive but emphasized that such a claim could only be demonstrated by direct investigations into mAbs. To our knowledge, only four mAbs that target glutamate-rich repeats have been described in which their epitopes have been determined. Of those mAbs, three were obtained following mouse immunization, and only one was of human origin. The murine mAbs 1A1 (53) and 1E10 (54) recognize Pf11.1-derived repeat peptides ($[PEE(L/V)VEEV(I/V)]_2$); the murine mAb 9B11 (55) is able to bind to a peptide containing four EENV repeats of RESA; and finally the human mAb 33G2 (56) is specific for a peptide repeat sequence found in Ag332 (VTEEI) (57). Despite all targeting linear epitopes containing tandem glutamate residues (EE), only 33G2 appeared to exhibit cross-reactivity (58) and none had been structurally characterized. Thus, our structure provides critical insights into how glutamate-rich-repeat targeting antibodies from immune individuals can cross-react with various *Pf* proteins expressed at different life cycle stages.

A most revealing observation from our structure is the presence of affinity-matured antibody-antibody homotypic interactions in the context of recognizing repetitive tandem glutamate residues present across the *Pf* proteome. The finding that B1E11K targets a repetitive epitope whilst engaging in affinity-matured homotypic interactions is similar to how antibodies elicited against repetitive elements of CSP can also bind through homotypic interactions (12) (14) (15) (13) (16) (19) (59) (17) (18) (11). We have previously shown that B cells expressing B cell receptors (BCRs) interacting via homotypic interactions activate more robustly in comparison to B cells that have mutated BCRs that disrupt this interaction (12). This strong B cell activation, presumably mediated through the cross-linking of multiple BCRs at the B cell surface (60), has been suggested to limit affinity maturation in germinal centers, potentially due to early exit of B cells, favouring the elicitation of short-term low-affinity antibodies to CSP over durable high-affinity responses, thus leading to suboptimal protective responses (61). However, this phenomenon may potentially be altered with the development of cross-reactive responses against repeats of slightly different content (62) (63) (64). Whether such insights extend to other anti-repeats antibody responses in general and anti-glutamate-rich repeats in particular remains largely unexplored.

Our observation of the recognition of RESA glutamate repeats by the B1E11K mAb through homotypic interactions tends to confirm a generalizable property of B cell responses to repetitive antigens where Abs can bind in close proximity. Here, we observed that B1E11K mAb exhibits a fair degree of somatic hypermutation and a relatively high affinity for RESA and cross-reactivity to other antigens. This finding provides further credence to the proposition that high affinity matured Abs to repeats can be elicited when cross-reacting to motifs of slightly different content, in the present case derived from antigens expressed at different stages of the *Pf* life cycle. Nonetheless, cross-binding to repeats-sharing proteins from different stages, as demonstrated with the B1E11K mAb, could also represent another mechanism by which repeated motifs may impact protective responses. Indeed, antibodies elicited by one protein with repeats may hinder subsequent potential protective responses to cross-recognized proteins expressed later in the parasite life cycle through antibody feedback mechanisms such as epitope masking (41) (65) (66) (67).

Ultimately, understanding the dynamics of how the immune system responds to repetitive elements could be critical for the future rational design of malaria vaccines. A desired characteristic for next-generation malaria vaccines will be the ability to elicit antibodies that can inhibit at multiple stages of the parasite's life cycle to prevent infection, reduce clinical manifestations, and lower the spread of the disease (68) (69). This could be accomplished by designing a multi-stage malaria vaccine that displays antigens expressed at various points of the parasite's life cycle. Utilizing glutamate-rich repeats in such a design may present benefits as a single antigen could potentially give rise to sera which contain antibodies that can both lower the clinical burden (asexual stage-targeting antibodies) and transmission of the disease (sexual stage-targeting antibodies). Indeed, antibodies elicited against the repetitive elements described here have been demonstrated to be associated with a lower incidence of disease (70) (71) (72) as well as disrupt the maturation of sexual stage parasites (53) in *in vitro* assays - although we note that mAb B1E11K isolated and characterized in this study did not show TRA.

As such, future work will be necessary to better understand the structure-activity relationships of mAbs targeting *Pf* repetitive elements across life cycle stages, such as the glutamate-rich repeats, and validate these targets as viable for next-generation malaria vaccines seeking the induction of long-lived immunity. The high-throughput target-agnostic approach used here has a strong potential for a further comprehensive exploration of humoral immunity to *Pf*.

Material and methods

PBMC sampling

(29)Donor A had lived in Central Africa for approximately 30 years and reported multiple malaria infections during that period. At the time of sampling PBMCs, Donor A had recently returned to the Netherlands and visited the hospital with a clinical malaria infection. After providing informed consent, PBMCs were collected, but gametocyte prevalence and density were not recorded.

Preparation of MBCs culture plates

Plates were prepared the day ahead of sorting and incubated at 37 °C. Three-hundred-eighty-four-well cell culture plates (Corning #CLS3570-50EA) were prepared with the appropriate memory B cell stimulation media one day before cell sorting, to allow the feeder cells sedimentation at the bottom of the wells. lscove's Modified Dulbecco's Medium (lMDM) (Gibco #12440061) was complemented with 1% penicillin-streptomycin (Thermo Fisher Scientific #10378016) and supplemented with 20% FBS (Gibco #16170-078). A cytokine cocktail was added to stimulate MBCs activation, with IL21 (Preprotech #200-21) at 100 ng/ml and IL2 (Preprotech#200-02) at 51 ng/ml. Fibroblasts expressing CD40L "L cells" (73) were irradiated at 50 Gy and 5000 were added in each well as feeder cells.

MBCs sorting

Cryopreserved PBMCs were thawed by a brief incubation in a 37 °C warm bath and stained with the following Miltenyi REA antibodies before sorting by flow cytometry: anti-CD3 (#130-114-519), anti-CD19 (#130-113-649), anti-CD20 (#130-113-649), anti-IgM (#130-113-476), anti-IgD (#130-110-643) and anti-IgA (#130-113-476). An Aqua LIVE/DEAD stain was also used (Thermo Fisher Scientific #L34957). Following staining, MBCs were sorted into the 384-well cell culture plates. After an 11 day culture period, supernatants were harvested using a pipetting robot (Eppendorf #5073) and transfered to storage plates (Greiner #788860-906). MBCs were lysed and their mRNA purified using the mRNA TurboCapture kit for 384 wells (Qiagen #72271). Lysates were stored at −80 °C. Lysates from selected wells were further transferred into 96-well RT-PCR plates (Biorad #HSP9641) to perform RT-PCR.

Gamete / gametocyte extract ELISA

Gamete or gametocyte lysate were prepared as described (27). Three hundred eighty four well plates (Thermo Fisher Scientific #460372) were coated with 7500 lysed gametes / gametocytes per well. Plates were incubated at 4°C overnight, then wells were washed three times with PBS-Tween 0.05%, prior to 1 hour blocking (with a 1% BSA - 1% PBS-Tween 0.05% solution). Cell culture supernatants (diluted ½ in blocking solution) were dispensed into the wells for a 1-hour incubation step. Following washing, secondary antibody (Thermo Fisher Scientific #A18814) diluted at 1/2000 was added and incubated for 1 h. Plates were then washed and 15 µl of CDP-substrate (Thermo Fisher Scientific #T2146) was added. The reaction was measured using Biotek Synergy 2 reader. Positivity threshold was determined as the average background OD + (3 x SD (background OD)). 0.3 µg/mL TB31F (anti-Pfs48/45 mAb), and 1.0 µg/mL 2544 (anti-*Pf*s25 mAb) were used as positive controls, while 30.0 µg/mL 399 (anti-CSP mAb) was used as negative control.

Monoclonal antibody isolation and production

Nested multiplexed PCRs were performed on single MBCs from selected wells following the protocol outlined by Tiller et al (37). PCR products were sent for sequencing (Genewiz®) and sequences analyzed for Ig gene features using the IMGT (ImMunoGeneTics) database (74). Ig

gene family-specific primers were used for cloning, as described by Tiller et al (PMID: 17996249) (37). Purified PCR products were cloned into vectors encoding for either IgG1 lambda, kappa or heavy constant regions. For transient mAb expression and secretion, HEK293 F cells were co-transfected with plasmids coding the Ab heavy chain and the corresponding light chain using 293 Fectin (TF#12347500). A protein A-Sepharose column (Sigma #ge17-1279-03) was used for mAb purification. Elution of mAbs was conducted with 4.5 ml of glycine 0.1 M (pH 2.5) and 500 µl of Tris 1 M (pH 9). The purified mAbs were subsequently subjected to buffer exchange and concentration with AmiconUltra (Merck #36100101).

Fab production

The DNA sequences of VK and VH of the B1E11K Fab domain were cloned upstream of human lgK and lgy1-CH1 domains respectively and inserted into a custom pcDNA3.4 expression vector. The plasmids were co-transfected into FreeStyle 293 F cells that were cultured in FreeStyle 293 Expression Media (Gibco #12338018) using Fectopro (Polyplus, 101000003). The recombinant Fab was purified via KappaSelect affinity chromatography (Cytiva #17545812) and cation exchange chromatography (MonoS, Cytiva 17516801).

Gamete surface immuno-fluorescence assay (SIFA)

Gamete SIFA was performed with *Pf* NF54 wild-typeand Pfs48/45 knockout (75) strains. The Pfs48/45 knockout lacks both surface-bound Pfs48/45 and Pfs230 (29) (35) (76)Wild-type or Pfs48/45 KO gametes were obtained following gametocyte activation in FBS for 1 h at room temperature. Gametes were washed with PBS and incubated with mAbs dilutions in PBS containing 0.5% PBS and 0.05% NaN_3 (SIFA buffer) for 1 hr at 4 °C in sterile V bottom plates (VWR#736-0223). After incubation, wells were washed three times with SIFA buffer and secondary antibody Alexa Fluor® 488 Goat Anti-Mouse IgG (H+L) (Invitrogen#A11001) diluted 1/200 added for a 1-hour incubation step on ice. Following a washing step, gametes were suspended in 4% paraformaldehyde and transferred into 384-well clear bottom black plates. Four images per well were taken using the ImageXpress® Pico Cell Imaging System (Molecular Devices).

Western blot

For western blots with gametocyte extract, *Pf* NF54 gametocyte extract was prepared as described above. The extract was mixed with NuPAGE™ LDS sample buffer (TF # NP0008) and heated for 15 min at 56 °C. The equivalent of 1 million lysed gametocytes was deposited per lane. A NuPAGE™ 4-12% Bis-Tris 2D-well gel (TF#NP0326BOX) was used for proteins separation. Using the Trans-Blot Turbo system (Bio-Rad #1704150) samples were then transferred to a 0.22 µm nitrocellulose membrane (Bio-Rad #1620150). The blots were cut into strips, blocked with 5% skimmed milk in PBS and incubated with 5 µg/ml of the mAb to be tested. Strips were incubated with the secondary anti-human IgG-HRP antibody (Pierce#31412), diluted 1/5000 in PBS-T. Clarity Western ECL substrate (Bio-Rad #1705060) was used for development and strips were imaged with the ImageQuant LAS4000 equipment (GE Healthcare).

For western blot with recombinant proteins, we used Pfs230CMB (amino acids 444-730) expressed in a plant-based transient expression system (77), and RESA3 (amino acids 570-1090), RESA (amino acids 66-585), LSA3 (amino acids 805-1558) and Pf11.1 (amino acids 3657-3734) that were expressed wheat germ cell free extract (*https://repository.ubn.ru.nl/bitstream/handle/2066/289602/289602.pdf?sequence=1*). All antigens contained a C-terminal His-tag. RESA and LSA3 also had an N-terminal GST-tag. The equivalent of 150 ng of protein was loaded per lane. An SDS 4-20% gel (BioRad # 4561094) was used for protein separation under non-reducing conditions. Further steps were performed following the protocol described above.

Recombinant Pfs48/45 and Pfs230 ELISA

ELISAs with full length Pfs48/45 and fragments thereof, and Pfs230CMB were performed as previously described (27) (77). In short, Nunc MaxiSorp 96-wells plates (ThermoFisher) were coated with 0.5 µg/mL recombinant Pfs48/45 or Pfs230CMB proteins, blocked with 5% skimmed milk in PBS + 0.1% Tween-20 and washed. Plates were then incubated with 10 or 30 µg/mL mAb in 1% skimmed milk in PBS. After washing, plates were incubated with 1:60,000 Goat anti-Human IgG/HRP-conjugated antibody (Pierce, Cat. No. 31412) in 1% skimmed milk in PBS + 0.1% Tween-20. After washing, plates were developed with 3,3',5,5'-Tetramethylbenzidine (TMB) and the reaction was stopped with H_2SO_4. Absorbance was measured at 450nm. mAbs were considered positive when the absorbance was higher than the mean absorbance plus three standard deviations of seven negative mAbs.

MAb poly-reactivity testing in ELISA

The coating antigens were diluted to 1 µg/ml. Antigens used were: ssDNA (Sigma #D8899-5MG), disialoganglioside GD1a (Sigma #G2392-1MG), lipopolysaccharide (Sigma #L2630-10MG), transferrin (Sigma #T3309-100MG), apotransferrin (Sigma #T1147-100MG), hemocyanin (Sigma #H7017-20MG), insulin (Sigma #I2643-25MG), cardiolipin (Sigma #C0563-10MG), albumin and histone (Sigma #H9250-100MG). Secondary antibody used was a phosphatase-coupled goat anti-human IgG (Jackson immuno #109 056 098). Optical densities were read at 405 nm, one hour after the addition of pNPP.

Standard Membrane Feeding Assay (SMFA)

SMFA experiments were performed using *Pf* NF54 wild-type gametocytes with oocyst count readout, following a protocol set up by Ponnudurai et al (78). Briefly, blood meals containing cultured gametocytes mixed with antibodies were fed to *A. stephensi* mosquitoes (Nijmegen colony). For each condition, 20 fully fed mosquitoes were analyzed. Reported antibody concentrations are concentrations in the total blood meal volume. mAbs that showed >80% transmission reducing activity (TRA), i.e. reduction in oocysts compared to a negative control, were tested in a second independent SMFA experiment. Transmission reducing activity (TRA) from one or two independent SMFA experiments was calculated using a negative binomial regression model as previously described (79). SMFA data analyses were done in R (version 4.1.2).

Microarray

Microarray design and protocol have been extensively detailed in (29) and (80). Briefly, selection proteins to be printed on the array was made on the basis of a systematic analyses of proteomic data by Meerstein-Kessel et al (81). In total 943 protein targets representing 528 unique gene IDs were expressed for the array using an in vitro transcription translation system; these were printed onto nitrocellulose coated slides at the University of California, Irvine as described previously (80). Microarray slides were rehydrated in blocking buffer (GVS #10485356) while B1E11K was diluted 1:100 in a 20% E. coli lysate/blocking buffer solution and incubated for 30 min. Blocking buffer was discarded and diluted B1E11K added to the array slides for incubation overnight at 4° C with continual rocking. Following three washes with TBS-Tween-20 0.05%, slides were probed with a fluorophore conjugated secondary antibody (Southern Biotech, Goat Anti-Human IgG-TXRD) at a concentration of 0.5 µg/mL (1:2000) in 2% E. coli lysate/blocking buffer solution. After three washes, slides were removed from their casettes and rinsed in ddH20air dried in a centrifuge and scanned using a GenePix 4300A High-resolution Microarray Scanner (Molecular Devices). Data treatment and analysis were performed using R (82). Correction for local array target spot background was done using the 'backgroundCorrect' function of the limma package (83). Background corrected values were log2 transformed and normalised to systematic effects by subtraction of the median signal intensity of the negative IVTT

controls (internally within four subarrays per sample). The final normalised data are a log2 MFI ratio of target to control reactivity: a value of 0 represents equality with the vehicle control, and a value of 1 indicates a signal twice as high.

Immunoprecipitation

Briefly, we used tosyl-activated beads (Invitrogen #14203) to covalently link B1E11K and incubated these beads with a gametocyte lysate to enable antigen capture. Immunoprecipitated antigens were eluted, and the elution fraction was run on an SDS-PAGE gel and silver-stained. A negative control immunoprecipitation experiment was performed using an anti-HIV gp120 mAb. As shown in sup Fig 2B, two bands with a molecular weight greater than 250 kDa, and a third one with a molecular weight around 55 kDa were specifically detected in the B1E11K immunoprecipitate, in comparison to the control antibody. The 3 bands were cut and sent for mass spectrometry analysis. Data were analyzed by querying the entire proteome of *Plasmodium falciparum* (NF54 isolate) in the Uniprot database.

Peptide synthesis

Peptides were produced by P. Verdié team, IBMM - SynBio3, Montpellier, France. Lyophilized peptides were solubilized in PBS.

ELISA with biotinylated peptides

ELISA protocol was similar to the protocol described above. Briefly, 96-well ELISA plates were coated overnight at 4° C with 0.5 µg/ml of streptavidin (TF # 434301). Plates were washed and then blocked for 1 h. Following wash, peptides diluted at 0.5 µg/ml were added to the plates for a 1 h incubation. The plates were washed and serially diluted mAbs were added. mAb fixation was detected using phosphatase-coupled goat anti-human IgG (Jackson Immuno #109 056 098) and para-nitrophenylphosphate (Interchim #UP 664791). The enzymatic reaction was measured at 405 nm using a TECAN Spark 10M plate reader. Half maximal effective concentration (EC50) was calculated from raw data (O.D) after normalization using GraphPad Prism (version 9) “log agonist versus normalized response” function.

BioLayer Interferometry (BLI) assay

All BLI experiments were performed using an Octet Red96e Instrument (PallForteBio), at 25°C and under 1000 rpm agitation. SAX biosensors (Sartorius # 18-5117) were pre-wetted in BLI Buffer [PBS (pH 7.4) + 0.01% (w/v) BSA + 0.002% (v/v) Tween-20] for 10 min. Biotinylated peptides were loaded onto the biosensors until the top concentration of B1E11K Fab utilized in kinetic assays (2500 nM for RESA 10 AA peptide and 625 nM for RESA P2 peptide) yielded a response value of ~ 1.2 nm. An association step was conducted by dipping the sensors into a titration series of ½ serially diluted B1E11K Fab for 30 seconds. The dissociation step was conducted by dipping the biosensors into BLI Buffer for 1200 seconds. Background subtractions were done using measurements where experiments were performed with biosensors treated in the same conditions but replacing Fab solution with BLI Buffer. Kinetic data were processed using the manufacturer’s software (Data analysis HT v11.1).

Isothermal Titration Calorimetry

An Auto-ITC200 (Malvern) was used to conduct calorimetric experiments. The RESA P2 peptide, RESA 10AA peptide, and recombinant B1E11K Fab were buffer-exchanged into Tris-buffered saline (20 mM Tris pH 7.0, and 150 mM NaCl). The B1E11K Fab was concentrated at 90 - 110 µM for experiments utilizing the RESA P2 peptide and 60 - 70 µM for those utilizing the RESA 10AA peptide. The RESA P2 peptide and RESA 10AA peptide were concentrated at 5-6 µM and 7-10 µM

respectively. Fab (syringe) was titrated into the cell (peptide) at 25°C using a protocol involving 19 injections each at a volume of 2.0 µL. The curves were fitted to a 2:1 or 1:1 binding model using the MicroCal ITC Origin 7.0 Analysis Software.

Size-Exclusion Chromatography-Multi-Angle Light Scattering (SEC-MALS)

SEC-MALS experiments were performed at 4°C using a Superdex 200 Increase 10/300 GL (Cytiva #GE17-5175-01) column. RESA P2 peptide was incubated with B1E11K Fab at a 1:6 molar ratio for 30 minutes prior to loading onto the Superdex 200 column. The column was set up onto an Agilent Technologies 1260 Infinity II HPLC coupled with a MiniDawn Treos MALS detector (Wyatt), Quasielastic light scattering (QELS) detector (Wyatt), and Optilab T-reX refractive index (RI) detector (Wyatt). Data processing was performed using the ASTRA software (Wyatt).

Negative Stain Electron Microscopy (nsEM) and Image Processing

Fractions of the first peak of the SEC-MALS experiments containing the 2:1 B1E11K:RESA P2 complex were used to make nsEM grids. 50 µg/mL of the complex was deposited onto homemade carbon film-coated grids (previously glow-discharged in air for 15s) and stained with 2% uranyl formate. Data was collected onto a Hitachi HT7800 microscope paired with an EMSIS Xarosa 20 Megapixel CMOS camera. Micrographs were taken with the microscope operating at 120 kV at 80,000x magnification with a pixel size of 1.83 Å/px. Image processing, particle picking, extractions, 2D classifications, and 3D reconstructions were done in cryoSPARC v2 (84).

X-Ray Crystallography and Structural Determination

The RESA P2 peptide was incubated with B1E11K Fab at a 1:5 molar ratio for 30 minutes prior to loading onto a Superdex 200 column Increase 10/300 GL column. Fractions containing the complex were pooled and concentrated at 8.6 mg/mL. A seed stock prepared from a previous crystallization trial was used for seeding. The stock was prepared from condition G9 of a JCSG Top96 screen (0.2M (NH4)2SO4 25% [w/v] PEG4000, and 0.1M sodium acetate [pH 4.6]). The complex, reservoir solution, and seed stock were mixed at a 3:4:1 volumetric ratio into an optimization tray derived from condition G9 of the JCSG Top96 screen. Crystals grew within 6 hours in a reservoir condition consisting of (0.1M NH4)2SO4 25% (w/v) PEG4000, and 0.1M sodium acetate (pH 5.2). Crystals were cryo-protected with 15% ethylene glycol (v/v) before being flash-frozen in liquid nitrogen. Data collection was performed at the 23-ID-B beamline at the Argonne National Laboratory Advanced Photon Source. Datasets were initially processed using autoproc (85) and further optimized using xdsgui (86). Molecular replacement was performed using PhaserMR (87) followed by multiple rounds of refinement using phenix.refine (88) and Coot (89). Inter- and intra-molecular contacts were determined using PISA (90) and manual inspection. Structural figures were generated using UCSF ChimeraX (91) (92).

Acknowledgements

We thank A. Guarino for her support to antibody production, N. Thielens for her input during the course of this work, Y. Couté for the proteomics analysis, J-B. Reiser for the preliminary BLI experiments, L. Chaperot for providing CD40L expressing fibroblasts, E. Thai and D. Ivanochko for their contributions to X-ray data collection and structure determination, K. Teelen for assistance with ELISAs, M. van de Vegte-Bolmer and R. Stoter for parasite culture, G.J. van Gemert and L. Pelser and A. Pouwelsen and J. Kuhnen and J. Klaassen and S. Mulder for mosquito rearing and dissection, and K. Koolen for support with ELISA and gamete binding experiments. Furthermore, we would like to thank Jessica Chichester (Fraunhofer) for providing Pfs230CMB. This work was supported in part by the Bill & Melinda Gates Foundation (OPP1108403). This work was also

undertaken, in part, thanks to funding from the Canadian Institutes for Health Research and was supported by the CIFAR Azrieli Global Scholar program (JPJ), the Ontario Early Researcher Award program (JPJ), and the Canada Research Chair program (JPJ). RY was supported by a Canada Graduate Scholarship - Master's (CGS-M). WS is supported by a Wellcome Trust Fellowship (218676/Z/19/Z). MMJ is supported by a Vidi grant from the Netherlands Organisation for Scientific Research (Vidi fellowship number 192.061). The proteomic experiments were partially supported by ANR grant ProFI (Proteomics French Infrastructure, ANR-10-INBS-08) and GRAL, a program from the Chemistry Biology Health (CBH) Graduate School of University Grenoble Alpes (ANR-17-EURE-0003). This work used the platforms of the Grenoble Instruct-ERIC center (ISBG; UAR 3518 CNRS-CEA-UGA-EMBL) within the Grenoble Partnership for Structural Biology (PSB), supported by FRISBI (ANR-10-INBS-0005-02) and GRAL, financed within the University Grenoble Alpes graduate school (Ecoles Universitaires de Recherche) CBH-EUR-GS (ANR-17-EURE-0003). Molecular graphics were generated using UCSF ChimeraX, developed by the Resource for Biocomputing, Visualization, and Informatics (University of California, San Francisco) with support from the National Institutes of Health (R01-GM129325) and the Office of Cyber Infrastructure and Computational Biology, National Institute of Allergy and Infectious Diseases.The BLI, ITC and SEC-MALS instruments were accessed at the Structural and Biophysical Core Facility, The Hospital for Sick Children, and EM data was collected at the Nanoscale Biomedical Imaging Facility, The Hospital for Sick Children, supported by the Canada Foundation for Innovation and Ontario Research Fund. X-ray diffraction experiments were in part performed using beamlines 23-ID-B at GM/CA@APS, which has been funded by the National Cancer Institute (ACB-12002) and the National Institute of General Medical Sciences (AGM-12006, P30GM138396). This research used resources of the Advanced Photon Source, a U.S. Department of Energy (DOE) Office of Science User Facility operated for the DOE Office of Science by Argonne National Laboratory under Contract No. DE-AC02-06CH11357. The Eiger 16M detector at GM/CA-XSD was funded NIH grant S10 OD012289. X-ray diffraction experiments were also performed using beamline AMX-17-ID-1 at the National Synchrotron Light Source II, a U.S. Department of Energy (DOE) Office of Science User Facility operated for the DOE Office of Science by Brookhaven National Laboratory under Contract No. DE-SC0012704. The Center for BioMolecular Structure (CBMS) is primarily supported by the National Institutes of Health, National Institute of General Medical Sciences (NIGMS) through a Center Core P30 Grant (P30GM133893), and by the DOE Office of Biological and Environmental Research (KP1607011). X-ray diffraction experiments were also performed using beamline CMCF-ID at the Canadian Light Source, a national research facility of the University of Saskatchewan, which is supported by the Canada Foundation for Innovation (CFI), the Natural Sciences and Engineering Research Council (NSERC), the National Research Council (NRC), the Canadian Institutes of Health Research (CIHR), the Government of Saskatchewan, and the University of Saskatchewan.

Competing Interests Statement

The authors declare to have no competing interests.

Author Contributions

A.A., R.Y, A.F-G., J.B. T.B., C.R.K., R.S.M., R.W.S, J-P.J., P.P. and M.M.J. designed research; A.A., R.Y., A.F-G., J.B., W.J.R.S., I.B., S.D-D., I.K., R.M.d.J. and M.d.B. performed research; A.A., R.Y., A.F-G., J.B., W.J.R.S., I.B., S.D-D., I.K., R.M.d.J., M.d.B. R.W.S., J-P.J., P.P. and M.M.J. analyzed data. A.A., R.Y. J-P.J., P.P. and M.M.J. wrote the original draft. All authors reviewed the manuscript.

References

1. (2021) **World malaria report 2021.**

2. Wicht KJ, Mok S, Fidock DA (2020) **Molecular Mechanisms of Drug Resistance in Plasmodium falciparum Malaria** *Annual Review of Microbiology* :431–54

3. Florens L, Washburn MP, Dale Raine J, Anthony RM, Graingerk M, David Haynes J, et al. (2002) **A proteomic view of the Plasmodium falciparum life cycle** *Nature*

4. Cowman AF, Healer J, Marapana D, Marsh K (2016) **Malaria: Biology and Disease** *Cell* **167**:610–24 https://doi.org/10.1016/j.cell.2016.07.055

5. Rosenberg R (2008) **Malaria: some considerations regarding parasite productivity** *Trends Parasitol* **24**:487–91

6. Laurens MB. (2019) **RTS,S/AS01 vaccine (MosquirixTM): an overview** *Hum Vaccin Immunother*

7. Datoo MS, Dicko A, Tinto H, Ouédraogo JB, Olotu A, Beaumont E, et al. (2023) **A phase III randomised controlled trial evaluating the malaria vaccine candidate R21/Matrix-MTM in African children** *SSRN*

8. Cerami C, Frevert U, Sinnis P, Takacs B, Clavijo P, Santos MJ, et al. (1992) **The Basolateral Domain of the Hepatocyte Plasma Membrane Bears Receptors for the Circumsporozoite Protein of Plasmodium falciparum Sporozoites** *Cell* **70**

9. Frevert U, Sinnis P, Cerami C, Shrefl W, Takacs B, Nussenzweig V (1993) **Malaria Circumsporozoite Protein Binds to Heparan Sulfate Proteoglycans Associated with the Surface Membrane of Hepatocytes** *J Exp Med*

10. Robert Ménard, Ali Sultan, Claudio Cortes, Rita Altszuler, Mélissa van Dijk, Chris Janse, et al. (1997) **Circumsporozoite protein is required for development of malaria sporozoites in mosquitoes** *Nature* **385**:336–40

11. Kucharska I, Thai E, Srivastava A, Rubinstein JL, Pomès R, Julien JP (2020) **Structural ordering of the plasmodium berghei circumsporozoite protein repeats by inhibitory antibody 3d11** *Elife* **9**:1–25

12. Imkeller K, Scally SW, Bosch A, Martí GP, Costa G, Triller G, et al. **Antihomotypic affinity maturation improves human B cell responses against a repetitive epitope**

13. Martin GM, Torres JL, Pholcharee T, Oyen D, Flores-Garcia Y, Gibson G, et al. (2023) **Affinity-matured homotypic interactions induce spectrum of PfCSP structures that influence protection from malaria infection** *Nat Commun* **14**

14. Pholcharee T, Oyen D, Flores-Garcia Y, Gonzalez-Paez G, Han Z, Williams KL, et al. (2021) **Structural and biophysical correlation of anti-NANP antibodies with in vivo protection against P. falciparum** *Nat Commun* **12**

15. Oyen D, Torres JL, Cottrell CA, Richter King C, Wilson IA, Ward AB (2018) **Cryo-EM structure of P. falciparum circumsporozoite protein with a vaccine-elicited antibody is stabilized by somatically mutated inter-Fab contacts** *Sci. Adv* **4**

16. Martin GM, Fernández-Quintero ML, Lee WH, Pholcharee T, Eshun-Wilson L, Liedl KR, et al. (2023) **Structural basis of epitope selectivity and potent protection from malaria by PfCSP antibody L9** *Nat Commun* **14**

17. Kucharska I, Hossain L, Ivanochko D, Yang Q, Rubinstein JL, Pomès R, et al. (2022) **Structural basis of Plasmodium vivax inhibition by antibodies binding to the circumsporozoite protein repeats** *Elife* **11**

18. Murugan R, Scally SW, Costa G, Mustafa G, Thai E, Decker T, et al. (2020) **Evolution of protective human antibodies against Plasmodium falciparum circumsporozoite protein repeat motifs** *Nature Medicine* **26**:1135–45

19. Tripathi P, Bender MF, Lei H, Da Silva Pereira L, Shen CH, Bonilla B, et al. (2023) **Cryo-EM structures of anti-malarial antibody L9 with circumsporozoite protein reveal trimeric L9 association and complete 27-residue epitope** *Structure* **31**:480–491

20. RTS,S Clinical Trials Partnership (2015) **Efficacy and safety of RTS,S/AS01 malaria vaccine with or without a booster dose in infants and children in Africa: Final results of a phase 3, individually randomised, controlled trial** *The Lancet* **386**:31–45

21. Wadman M (2023) **First malaria vaccine slashes childhood deaths** *Science* **382**:357–357

22. Golumbeanu M, Yang GJ, Camponovo F, Stuckey EM, Hamon N, Mondy M, et al. (2022) **Leveraging mathematical models of disease dynamics and machine learning to improve development of novel malaria interventions** *Infect Dis Poverty* **11**

23. Stone WJR, Dantzler KW, Nilsson SK, Drakeley CJ, Marti M, Bousema T, et al. (2016) **Naturally acquired immunity to sexual stage P. Falciparum parasites** *Parasitology* :187–98

24. Duffy PE (2021) **Transmission-Blocking Vaccines: Harnessing Herd Immunity for Malaria Elimination** *Expert Review of Vaccines* :185–98

25. Roeffen W, Teelen K, Van As J, Vd Vegte-Bolmer M, Eling W, Sauerwein R (2001) **Plasmodium falciparum: Production and characterization of rat monoclonal antibodies specific for the sexual-stage Pfs48/45 antigen** *Exp Parasitol* **97**:45–9

26. Ivanochko D, Fabra-García A, Teelen K, van de Vegte-Bolmer M, van Gemert GJ, Newton J, et al. (2023) **Potent transmission-blocking monoclonal antibodies from naturally exposed individuals target a conserved epitope on Plasmodium falciparum Pfs230** *Immunity* **56**:420–432

27. Fabra-García A, Hailemariam S, de Jong RM, Janssen K, Teelen K, van de Vegte-Bolmer M, et al. (2023) **Highly potent, naturally acquired human monoclonal antibodies against Pfs48/45 block Plasmodium falciparum transmission to mosquitoes** *Immunity* **56**:406–419

28. Kundu P, Semesi A, Jore MM, Morin MJ, Price VL, Liang A, et al. (2018) **Structural delineation of potent transmission-blocking epitope I on malaria antigen Pfs48/45** *Nat Commun* **9**

29. Stone WJR, Campo JJ, Ouédraogo AL, Meerstein-Kessel L, Morlais I, Da D, et al. (2018) **Unravelling the immune signature of Plasmodium falciparum transmission-reducing immunity** *Nat Commun* **9**

30. Coelho CH, Tang WK, Burkhardt M, Galson JD, Muratova O, Salinas ND, et al. (2021) **A human monoclonal antibody blocks malaria transmission and defines a highly conserved neutralizing epitope on gametes** *Nat Commun* **12**

31. Tang WK, Coelho CH, Miura K, Nguemwo Tentokam BC, Salinas ND, Narum DL, et al. (2023) **A human antibody epitope map of Pfs230D1 derived from analysis of individuals vaccinated with a malaria transmission-blocking vaccine** *Immunity* **56**:433–443

32. Ko KT, Lennartz F, Mekhaiel D, Guloglu B, Marini A, Deuker DJ, et al. (2022) **Structure of the malaria vaccine candidate Pfs48/45 and its recognition by transmission blocking antibodies** *Nat Commun* **13**

33. Lennartz F, Brod F, Dabbs R, Miura K, Mekhaiel D, Marini A, et al. (2018) **Structural basis for recognition of the malaria vaccine candidate Pfs48/45 by a transmission blocking antibody** *Nat Commun* **9**

34. Singh K, Burkhardt M, Nakuchima S, Herrera R, Muratova O, Gittis AG, et al. (2020) **Structure and function of a malaria transmission blocking vaccine targeting Pfs230 and Pfs230-Pfs48/45 proteins** *Commun Biol* **3**

35. Eksi S, Czesny B, Van Gemert GJ, Sauerwein RW, Eling W, Williamson KC (2006) **Malaria transmission-blocking antigen, Pfs230, mediates human red blood cell binding to exflagellating male parasites and oocyst production** *Mol Microbiol* **61**:991–8

36. Brooks SR, Williamson KC (2000) **Proteolysis of Plasmodium falciparum surface antigen, Pfs230, during gametogenesis** *Molecular and Biochemical Parasitology* **106**

37. Tiller T, Meffre E, Yurasov S, Tsuiji M, Nussenzweig MC, Wardemann H (2008) **Efficient generation of monoclonal antibodies from single human B cells by single cell RT-PCR and expression vector cloning** *J Immunol Methods* **329**:112–24

38. Kundu P, Semesi A, Jore MM, Morin MJ, Price VL, Liang A, et al. (2018) **Structural delineation of potent transmission-blocking epitope I on malaria antigen Pfs48/45** *Nat Commun* **9**

39. Coelho CH, Tang WK, Burkhardt M, Galson JD, Muratova O, Salinas ND, et al. (2021) **A human monoclonal antibody blocks malaria transmission and defines a highly conserved neutralizing epitope on gametes** *Nat Commun [Internet* :1–12 https://doi.org/10.1038/s41467-021-21955-1

40. Hou N, Jiang N, Ma Y, Zou Y, Piao X, Liu S, et al. (2020) **Low-Complexity Repetitive Epitopes of Plasmodium falciparum Are Decoys for Humoural Immune Responses** *Front Immunol* **11**

41. Raghavan M, Kalantar KL, Duarte E, Teyssier N, Takahashi S, Kung AF, et al. (2023) **Proteome-wide antigenic profiling in Ugandan cohorts identifies associations between age, exposure intensity, and responses to repeat-containing antigens in Plasmodium falciparum** *Elife* **12**

42. Cardoso RMF, Zwick MB, Stanfield RL, Kunert R, Binley JM, Katinger H, et al. (2005) **Broadly neutralizing anti-HIV antibody 4E10 recognizes a helical conformation of a highly conserved fusion-associated motif in gp41** *Immunity* **22**:163–73

43. Heger A, Holm L (2000) **Rapid Automatic Detection and Alignment of Repeats in Protein Sequences** *Proteins*

44. Williamsona KC, Fujiokab H, Aikawab M, Kaslowc DC (1996) **Stage-specific processing of Pfs230, a Plasmodium falciparum transmission-blocking vaccine candidate** *Molecular and Biochemical Parasitology* **78**

45. De Jong RM (2023) **Towards efficacious transmission blocking malaria vaccines The long and winding path** *Towards efficacious transmission blocking malaria vaccines*

46. Kratochvil S, Shen CH, Lin YC, Xu K, Nair U, Da Silva Pereira L, et al. (2021) **Vaccination in a humanized mouse model elicits highly protective PfCSP-targeting anti-malarial antibodies** *Immunity* **54**:2859–2876

47. Ye J, Ma N, Madden TL, Ostell JM (2013) **IgBLAST: an immunoglobulin variable domain sequence analysis tool** *Nucleic Acids Res* **41**

48. Miura K, Takashima E, Pham TP, Deng B, Zhou L, Huang WC, et al. (2022) **Elucidating functional epitopes within the N-terminal region of malaria transmission blocking vaccine antigen Pfs230** *NPJ Vaccines* **7**

49. Simons LM, Ferrer P, Gombakomba N, Underwood K, Herrera R, Narum DL, et al. (2023) **Extending the range of Plasmodium falciparum transmission blocking antibodies** *Vaccine* **41**:3367–79

50. Inklaar MR, de Jong RM, Bekkering ET, Nagaoka H, Fennemann FL, Teelen K, et al. (2023) **Pfs230 Domain 7 is targeted by a potent malaria transmission-blocking monoclonal antibody** *NPJ Vaccines* **8**

51. de Jong RM, Meerstein-Kessel L, Da DF, Nsango S, Challenger JD, van de Vegte-Bolmer M, et al. (2021) **Monoclonal antibodies block transmission of genetically diverse Plasmodium falciparum strains to mosquitoes** *npj Vaccines. Nature Research* **6**

52. Simon N, Kuehn A, Williamson KC, Pradel G (2016) **Adhesion protein complexes of malaria gametocytes assemble following parasite transmission to the mosquito** *Parasitol Int* **65**:27–30

53. Feng Z, Hoffmann KN, Nussenzweig RS, Tsuji M, Fujioka H, Aikawa M, et al. (1993) **Pfs2400 Can Mediate Antibody-dependent Malaria Transmission Inhibition and May Be the Plasmodium Falciparum 11.1 Gene Product** *J Exp Med.*

54. Scherf A, Carter' R, Petersen2 C, Alano3 P, Nelson2 R, Aikawa4 M, et al. (1992) **Gene inactivation of Pf 11-1 of Plasmodium falciparum by chromosome breakage and healing: identification of a gametocyte-specific protein with a potential role in gametogenesis** *The EMBO Journal* **1**

55. Masuda A, Zavala F, Nussenzweig V, Nussenzweig RS (1986) **Monoclonal anti-gametocyte antibodies identify an antigen present in all blood stages of Plasmodium faIciparum** *Molecular and Biochemical Parasitology* **19**

56. Rachanee Udomsangpetch, Katarina Lundgren, Klaus Berzins, Birgitta Wahlin, Hedvig Perlmann, Marita Troye-Blomberg, et al. (1986) **Human monoclonal antibodies to Pf 155 a major antigen of malaria parasite Plasmodium falciparum** *Science*

57. Ahlborg N, Berzins K, Perlmann P (1991) **Definition of the epitope recognized by the Plasmodiumfalciparum-reactive human monoclonal antibody 33G2** *Molecular and Biochemical Parasitology* **46**

58. Rachanee Udomsangpetch, Jan Carlsson, Birgitta Wahlin, Goran Holmquist, Luiz Ozaki, Arthur Scherf, et al. (2018) **Reactivity of the human monoclonal antibody 33G2 with repeated sequences of three distinct Plasmodium falciparum antigens** *J Immunol*

59. Kucharska T, Binter S, Murugan R, Scally SW, Ludwig J, Prieto K, et al. (2022) **High-density binding to Plasmodium falciparum circumsporozoite protein repeats by inhibitory antibody elicited in mouse with human immunoglobulin repertoire** *PLoS Pathog* **18**

60. Clutterbuck EA, Lazarus R, Yu LM, Bowman J, Bateman EAL, Diggle L, et al. (2012) **Pneumococcal conjugate and plain polysaccharide vaccines have divergent effects on antigen-specific B cells** *Journal of Infectious Diseases* **205**:1408–16

61. Wahl I, Wardemann H (2022) **How to induce protective humoral immunity against Plasmodium falciparum circumsporozoite protein** *Journal of Experimental Medicine*

62. Murugan R, Scally SW, Costa G, Mustafa G, Thai E, Decker T, et al. (2020) **Evolution of protective human antibodies against Plasmodium falciparum circumsporozoite protein repeat motifs** *Nat Med* **26**:1135–45

63. Ludwig J, Scally SW, Costa G, Hoffmann S, Murugan R, Lossin J, et al. (2023) **Glycosylated nanoparticle-based PfCSP vaccine confers long-lasting antibody responses and sterile protection in mouse malaria model** *NPJ Vaccines* **8**

64. Thai E, Murugan R, Binter S, Burn Aschner C, Prieto K, Kassardjian A, et al. (2023) **Molecular determinants of cross-reactivity and potency by VH3-33 antibodies against the Plasmodium falciparum circumsporozoite protein** *Cell Rep [Internet* **42**

65. Chatterjee D, Lewis FJ, Sutton HJ, Kaczmarski JA, Gao X, Cai Y, et al. (2021) **Avid binding by B cells to the Plasmodium circumsporozoite protein repeat suppresses responses to protective subdominant epitopes** *Cell Rep* **35**

66. Chatterjee D, Cockburn IA (2021) **The challenges of a circumsporozoite protein-based malaria vaccine** *Expert Rev Vaccines* **20**:113–25

67. McNamara HA, Idris AH, Sutton HJ, Vistein R, Flynn BJ, Cai Y, et al. (2020) **Antibody Feedback Limits the Expansion of B Cell Responses to Malaria Vaccination but Drives Diversification of the Humoral Response** *Cell Host Microbe* **28**:572–585

68. Nahrendorf W, Scholzen A, Sauerwein RW, Langhorne J (2015) **Cross-stage immunity for malaria vaccine development** *Vaccine* **33**:7513–7

69. Julien JP, Wardemann H (2019) **Antibodies against Plasmodium falciparum malaria at the molecular level** *Nature Reviews Immunology. Nature Research* **19**:761–75

70. Riley EM, Allen SJ, Troye-Blomberg M, Bennett S, Perlmann H, Andersson G, et al. (1991) **Association between immune recognition of the malaria vaccine candidate antigen Pf155/RESA and resistance to clinical disease: a prospective study in a malaria-endemic region of West Africa** *Trans R Soc Trop Med Hyg* **85**:436–43 https://doi.org/10.1016/0035-9203(91)90207-F

71. Petersen E, Høgh B, Marbiah NT, Perlmann H, Willcox M, Dolopaie E, et al. (1990) **A longitudinal study of antibodies to the Plasmodium falciparum antigen Pf155/RESA and immunity to malaria infection in adult Liberians** *Trans R Soc Trop Med Hyg* **84**:339–45 https://doi.org/10.1016/0035-9203(90)90307-Z

72. Berzins K, Perlmann H, Wahlin B, Ekre HP, Hogh B, Petersen E, et al. (1991) **Passive Immunization of Aotus Monkeys with Human Antibodies to the Plasmodium falciparum Antigen Pfl55/RESA** *Infection and immunity* **59**

73. Garrone P, Neidhardt EM, Garcia E, Galibert L, Van Kooten C, Banchereau J (1995) **Fas Ligation Induces Apoptosis of CD40-activated Human B Lymphocytes** *J Exp Med.*

74. Lefranc MP, Giudicelli V, Duroux P, Jabado-Michaloud J, Folch G, Aouinti S, et al. (2015) **IMGT R, the international ImMunoGeneTics information system R 25 years on** *Nucleic Acids Res* **43**:D413–22

75. Van Dijk MR, Janse CJ, Thompson J, Waters AP, Braks JAM, Dodemont HJ, et al. (2001) **A Central Role for P48/45 in Malaria Parasite Male Gamete Fertility The central role of zygote formation in the life cycle and transmission of the parasite makes gametes and** *Cell* **104**

76. Nirbhay KUMAR (1987) **Target antigens of malaria transmission blocking immunity exist as a stable membrane bound complex** *Parasite Immunology* **9**

77. Farrance CE, Rhee A, Jones RM, Musiychuk K, Shamloul M, Sharma S, et al. (2011) **A plant-produced Pfs230 vaccine candidate blocks transmission of Plasmodium falciparum** *Clinical and Vaccine Immunology* **18**:1351–7

78. Ponnudurai T, Lensen AHW, Van Gemert GJA, Bensink MPE, Bolmer M, Meuwissen JHET (1989) **Infectivity of cultured Plasmodium falciparum gametocytes to mosquitoes** *Parasitology* **98**:165–73

79. de Jong RM, Singh SK, Teelen K, van de Vegte-Bolmer M, van Gemert GJ, Stone WJR, et al. (2022) **Heterologous Expression and Evaluation of Novel Plasmodium falciparum Transmission Blocking Vaccine Candidates** *Front Immunol* **13**

80. de Jong RM, Alkema M, Oulton T, Dumont E, Teelen K, Nakajima R, et al. (2022) **The acquisition of humoral immune responses targeting Plasmodium falciparum sexual stages in controlled human malaria infections** *Front Immunol* **13**

81. Meerstein-Kessel L, Van Der Lee R, Stone W, Lanke K, Baker DA, Alano P, et al. (2018) **Probabilistic data integration identifies reliable gametocyte-specific proteins and transcripts in malaria parasites** *Sci Rep* **8**

82. Staples TL (2023) **Expansion and evolution of the R programming language** *R Soc Open Sci* **10**

83. Ritchie ME, Phipson B, Wu D, Hu Y, Law CW, Shi W, et al. (2015) **Limma powers differential expression analyses for RNA-sequencing and microarray studies** *Nucleic Acids Res* **43**

84. Punjani A, Rubinstein JL, Fleet DJ, Brubaker MA (2017) **cryoSPARC: algorithms for rapid unsupervised cryo-EM structure determination** *Nature Methods* **14**:290–6

85. Vonrhein C, Flensburg C, Keller P, Sharff A, Smart O, Paciorek W, et al. (2011) **Data processing and analysis with the autoPROC toolbox** *Acta Crystallogr D Biol Crystallogr* **67**:293–302

86. Kabsch W (2010) **XDS** *Acta Crystallogr D Biol Crystallogr [Internet]* **66**:125–32

87. McCoy AJ, Grosse-Kunstleve RW, Adams PD, Winn MD, Storoni LC, Read RJ (2007) **Phaser crystallographic software** *J Appl Crystallogr* **40**:658–74

88. Liebschner D, Afonine P V., Baker ML, Bunkoczi G, Chen VB, Croll TI, et al. (2019) **Macromolecular structure determination using X-rays, neutrons and electrons: Recent developments in Phenix** *Acta Crystallogr D Struct Biol* **75**:861–77

89. Emsley P, Lohkamp B, Scott WG, Cowtan K (2010) **Features and development of Coot** *Acta Crystallogr D Biol Crystallogr* **66**:486–501

90. Krissinel E, Henrick K (2007) **Inference of Macromolecular Assemblies from Crystalline State** *J Mol Biol* **372**:774–97

91. Goddard TD, Huang CC, Meng EC, Pettersen EF, Couch GS, Morris JH, et al. (2018) **UCSF ChimeraX: Meeting modern challenges in visualization and analysis** *Protein Science* **27**:14–25

92. Pettersen EF, Goddard TD, Huang CC, Meng EC, Couch GS, Croll TI, et al. (2021) **UCSF ChimeraX: Structure visualization for researchers, educators, and developers** *Protein Science* **30**:70–82

Editors

Reviewing Editor
Urszula Krzych
Walter Reed Army Institute of Research, Silver Spring, United States of America

Senior Editor
Dominique Soldati-Favre
University of Geneva, Geneva, Switzerland

Reviewer #2 (Public Review):

This manuscript by Amen, Yoo and Fabra-Garcia et al describes a human monoclonal antibody B1E11K, targeting EENV repeats which are present in parasite antigens such as Pfs230, RESAs and Pf11.1. The authors isolated B1E11K using an initial target agnostic approach for antibodies that would bind gamete/gametocyte lysate which they made 14 mAbs. Following a suite of highly appropriate characterization methods from Western blotting of recombinant proteins to native parasite material, use of knockout lines to validate specificity, ITC, peptide mapping, SEC-MALS, negative stain EM and crystallography, the authors have built a compelling case that B1E11K does indeed bind EENV repeats. In addition, using X-ray crystallography they show that two B1E11K Fabs bind to a 16 aa RESA repeat in a head-to-head conformation using homotypic interactions and provide a separate example from CSP, of affinity-matured homotypic interactions.

The authors have addressed most of our previous comments in their revised manuscript.

One of the main conclusions in the paper is the binding of B1E11K to RESAs which are blood stage antigens that are exported to the infected parasite surface. In the future, it would be interesting to understand if B1E11K mAb binds to the red cell surface of infected blood stage parasites to understand its cellular localization in those stages.

Materials and Methods:
PBMC sampling: While the authors have provided clarification that they obtained informed consent from the PBMC donor, they have not added the ethics approval codes in this section.

https://doi.org/10.7554/eLife.97865.2.sa2

Reviewer #3 (Public Review):

The manuscript from Amen et al reports the isolation and characterization of human antibodies that recognize proteins expressed at different sexual stages of Plasmodium falciparum. The isolation approach was antigen agnostic and based on the sorting, activation, and screening of memory B cells from a donor whose serum displays high transmission-reducing activity. From this effort, 14 antibodies were produced and further characterized. The antibodies displayed a range of transmission-reducing activities and recognized different Pf sexual stage proteins. However, none of these antibodies had substantially higher TRA than previously described antibodies.

The authors then performed further characterization of antibody B1E11K, which was unique in that it recognized multiple proteins expressed during sexual and asexual stages. Using protein microarrays, B1E11K was shown to recognize glutamate-rich repeats, following an EE-XX-EE pattern. An impressive set of biophysical experiments were performed to extensively characterize the interactions of B1E11K with various repeat motifs and lengths. Ultimately, the authors succeeded in determining a 2.6 A resolution crystal structure of B1E11K bound to a 16AA repeat-containing peptide. Excitingly, the structure revealed that two Fabs bound simultaneously to the peptide and made homotypic antibody-antibody contacts. This had only previously been observed before with antibodies directed against CSP repeats.

Overall I found the manuscript to be very well written. Strengths of the manuscript include the target-agnostic screening approach and the thorough characterization of antibodies. The demonstration that B1E11K is cross-reactive to multiple proteins containing glutamate-rich repeats, and that the antibody recognizes the repeats via homotypic interactions, similar to what has been observed for CSP repeat-directed antibodies, should be of interest to many in the field.

https://doi.org/10.7554/eLife.97865.2.sa1

Author response:

The following is the authors' response to the original reviews.

> ***Public Reviews:***
>
> ***Reviewer #1 (Public Review):***
>
> *Summary:*
>
> *In this paper, the authors used target agnostic MBC sorting and activation methods to identify B cells and antibodies against sexual stages of Plasmodium falciparum. While they isolated some Mabs against PFs48/45 and PFs230, two well-known candidates for "transmission blocking" vaccines, these antibodies' efficacies, as measured by TRA, did not perform as well as other known antibodies. They also isolated one cross-reactive mAb to proteins containing glutamic acid-rich repetitive elements, that express at different stages of the parasite life cycle. They then determined the structure of the Fab with the*

> *highest protein binder they could determine through protein microarray, RESA, and observed homotypic interactions.*
>
> *Strengths:*
>
> *- Target agnostic B cell isolation (although not a novel methodology).*
>
> *- New cross-reactive antibody with some "efficacy" (TRA) and mechanism (homotypic interactions) as demonstrated by structural data and other biophysical data.*
>
> *Weaknesses:*
>
> *The paper lacks clarity at times and could benefit from more transparency (showing all the data) and explanations.*

We have added the oocyst count data from the SMFA experiments as Supplementary Table 2, and ELISA binding curves underlying Figure 4B as Supplementary Figure 5.

> *In particular:*
>
> *- define SIFA*
>
> *- define TRAbs*

We have carefully gone through the manuscript and have introduced abbreviations at first use, removed unnecessary abbreviations and removed unnecessary jargon to increase readability.

> *- it is not possible to read the Figure 6B and C panels.*

We regret that the labels in Supplementary Figures 6 and 7 were of poor quality and have now included higher resolution images to solve this issue.

> ***Reviewer #2 (Public Review):***
>
> *This manuscript by Amen, Yoo, Fabra-Garcia et al describes a human monoclonal antibody B1E11K, targeting EENV repeats which are present in parasite antigens such as Pfs230, RESAs, and 11.1. The authors isolated B1E11K using an initial target agnostic approach for antibodies that would bind gamete/gametocyte lysate which they made 14 mAbs. Following a suite of highly appropriate characterization methods from Western blotting of recombinant proteins to native parasite material, use of knockout lines to validate specificity, ITC, peptide mapping, SEC-MALS, negative stain EM, and crystallography, the authors have built a compelling case that B1E11K does indeed bind EENV repeats. In addition, using X-ray crystallography they show that two B1E11K Fabs bind to a 16 aa RESA repeat in a head-to-head conformation using homotypic interactions and provide a separate example from CSP, of affinity-matured homotypic interactions.*
>
> *There are some minor comments and considerations identified by this reviewer, These include that one of the main conclusions in the paper is the binding of B1E11K to RESAs which are blood stage antigens that are exported to the infected parasite surface. It would have been interesting if immunofluorescence assays with B1E11K mAb were performed with blood-stage parasites to understand its cellular localization in those stages.*

In the current manuscript, we provide multiple lines of evidence that B1E11K binds (with high affinity) to repeats that are present in RESAs, i.e. through micro-array studies, in vitro

binding experiments such as Western blot, ELISA and BLI, and through X-ray crystallography studies on B1E11k – repeat peptide complexes. Taken together, we think we provide compelling evidence that B1E11k binds to repeats present in RESA proteins. We do agree that studies on the function of this mAb against other stages of the parasite could be of interest, but as our manuscript focuses on the sexual stage of the parasite, we feel that this is beyond scope of the current work. However, this line of inquiry will be strongly considered in follow up studies.

> ***Reviewer #3 (Public Review):***
>
> *The manuscript from Amen et al reports the isolation and characterization of human antibodies that recognize proteins expressed at different sexual stages of Plasmodium falciparum. The isolation approach was antigen agnostic and based on the sorting, activation, and screening of memory B cells from a donor whose serum displays high transmission-reducing activity. From this effort, 14 antibodies were produced and further characterized. The antibodies displayed a range of transmission-reducing activities and recognized different Pf sexual stage proteins. However, none of these antibodies had substantially lower TRA than previously described antibodies.*
>
> *The authors then performed further characterization of antibody B1E11K, which was unique in that it recognized multiple proteins expressed during sexual and asexual stages. Using protein microarrays, B1E11K was shown to recognize glutamate-rich repeats, following an EE-XX-EE pattern. An impressive set of biophysical experiments was performed to extensively characterize the interactions of B1E11K with various repeat motifs and lengths. Ultimately, the authors succeeded in determining a 2.6 A resolution crystal structure of B1E11K bound to a 16AA repeat-containing peptide. Excitingly, the structure revealed that two Fabs bound simultaneously to the peptide and made homotypic antibody-antibody contacts. This had only previously been observed with antibodies directed against CSP repeats.*
>
> *Overall I found the manuscript to be very well written, although there are some sections that are heavy on field-specific jargon and abbreviations that make reading unnecessarily difficult. For instance, 'SIFA' is never defined.*

We have carefully gone through the manuscript and have introduced abbreviations at first use, removed unnecessary abbreviations and removed unnecessary jargon to increase readability.

> *Strengths of the manuscript include the target-agnostic screening approach and the thorough characterization of antibodies. The demonstration that B1E11K is cross-reactive to multiple proteins containing glutamate-rich repeats, and that the antibody recognizes the repeats via homotypic interactions, similar to what has been observed for CSP repeat-directed antibodies, should be of interest to many in the field.*
>
> ***Recommendations for the authors:***
>
> ***Reviewer #1 (Recommendations For The Authors):***
>
> *Figure 1 - why only gametes ELISA and Spz or others?*

The volumes of the single B cell supernatants were too small to screen against multiple antigens/parasite stages. As we aimed to isolate antibodies against the sexual stages of the parasite, our assay focused on this stage and supernatants were not tested against other stages. Furthermore, we screened for reactivity against gametes as TRA mAbs likely target gametes rather than other forms of sexual stage parasites.

> *Figure 2 A*
>
> *(a) Wild type (WT) and Pfs48/45 knock-out (KO) gametes.*
>
> *(b) I am a bit confused about what GMT is vs Pfs48/45*

We have changed the column titles in Figure 2A to “wild-type gametes” and “Pfs48/45 knockout gametes” to improve clarity.

> *(c) Binding is high % why is it red?*

We chose to present the results in a heatmap format with a graded color scale, from strong binders in red to weak binders in green. It has now been clarified in the legend of the figure.

> *Please state acronyms clearly*
>
> *TRA - transmission reducing activity*
>
> *SMFA - standard membrane feeding assay*

We have added the full terms to clarify the acronyms.

> *1123- VRC01 (not O1)*

We have corrected this.

> *Figure 2 C bottom panels, clarify which ones are TRAbs (Assuming the Mabs with over 80% TRA at 500 ug/ml) (right gel) and the ones that are not (left gel)?*

In the Western blot in Figure 2c, we have marked the antibodies with >80% TRA with an asterisk.

Furthermore, we have replaced ‘TRAbs’ by ‘mAbs with >80% TRA at 500 µg/mL’ in the figure legend.

> *ITC show the same affinity of the Fab to the 2 peptides but not the ELISA, not the BLI/SPR would be more appropriate. Any potential explanation?*

The way binding affinity is determined across various techniques can result in slight differences in determined values. For instance, ELISAs utilize long incubation times with extensive washing steps and involve a spectroscopic signal, isothermal titration calorimetry (ITC) uses calorimetric signal at different concentration equilibriums to extract a KD, and BLI determines kinetic parameters for KD determination. Discrepancies in binding affinities between orthologous techniques have indeed been observed previously in the context of peptide-antibody binding (e.g. PMID: 34788599).

Despite this, regardless of technique, the relative relationships in all three sets of data is the same - higher binding affinity is observed to the longer P2 peptide. This is the main takeaway of the section. As the reviewer suggests, BLI is likely the most appropriate readout here and is the only value explicitly mentioned in the main text. We primarily use ITC to support our proposed binding stoichiometry which is important to substantiate the SEC-MALS and nsEM data in Figure 4H-I. We added the following sentences to help reinforce these points: “The determined binding affinity from our ITC experiments (Table 1) differed from our BLI experiments (Fig. 4D and 4E), which can occur when measuring antibody-peptide

interactions. Regardless, our data across techniques all trend toward the same finding in which a stronger binding affinity is observed toward the longer RESA P2 (16AA) peptide."

> *Figure 5C - would be helpful to have the peptide sequence above referring to what is E1, E2 etc...*

We added two panels (Figure 5C-D) showcasing the binding interface that shows the peptide numbering in the context of the overall complex. We hope that this will help better orient the reader.

> *Figure S4 - maybe highlight in different colors the EENVV, EEIEE, Etc, etc*

Repeats found in the sequence of the various proteins in Figure S4 have now been highlighted with different colors.

> *Line 163 - why 14 mabs if 11 wells? Isn't it 1 B cell per well? The authors should explain right away that some wells have more than 1 B cell and some have 1 HC, 1LC, and 1 KC.*

We agree that this was somewhat confusing and have modified the text which now reads: "We obtained and cloned heavy and light chain sequences for 11 out of 84 wells. For three wells we obtained a kappa light chain sequence and for five wells a lambda light chain sequence. For three wells we obtained both a lambda and kappa light chain sequence suggesting that either both chains were present in a single B cell or that two B cells were present in the well. For all 14 wells we retrieved a single heavy chain sequence. Following amplification and cloning, 14 mAbs, from 11 wells, were expressed as full human IgG1s (Table S1) (Dataset S1)."

> *Line 166-167 - were they multiple HC (different ones) as well when Lambda and kappa were present?*
>
> *This is not clear at first.*

We clarified this point in the text, see also comment above.

> *Line 177 - expressed Pfs48/45 and Pfs230, is it lacking both or just Pfs48/45 (as stated on line 172)?*

Pfs48/45 binds to the gamete surface via a GPI anchor, while Pfs230 is retained to the surface through binding to Pfs48/45. Hence, the Pfs48/45 knockout parasite will therefore also lack surfacebound Pfs230. We have added a sentence to the Results clarifying this: "The mAbs were also tested for binding to Pfs48/45 knock-out female gametes, which lack surface-bound Pfs48/45 and Pfs230".

> *Show the ELISA data used to calculate EC50 in Figure 3.*

ELISA binding curves are now shown as Figure S5.

> *Line 313-315 - what if you reverse, capture the Fab (peptide too small even if biotinylated?)*

As anticipated by the Reviewer, immobilizing the Fab and dipping into peptide did not yield appreciable signal for kinetic analysis and thus the experiment from this setup is not reported.

> *Line 341 - add crystal structure*

This has now been added.

> *There is a bit too much speculation in the discussion. For e.g. "The B1C5L and B1C5K mAbs were shown to recognize Domain 2 of Pfs48/45 and exhibited moderate potency, as previously described for Abs with such specificity (27). These 2 mAbs were isolated from the same well and shared the same heavy chain; their three similar characteristics thus suggest that their binding is primarily mediated by the heavy chain". Actual data will reinforce this statement.*

As B1C5L and B1C5K recognized domain 2 of Pfs48/45 with similar affinity, this strongly suggests that binding is mediated though the heavy chain. Structural analysis could confirm this statement, but this is out of the scope of this study.

> ***Reviewer #2 (Recommendations For The Authors):***
>
> *Figure 1: This figure provides a description of the workflow. To make it more relevant for the paper, the authors could add relevant numbers as the workflow proceeds.*
>
> *(a) For example, how many memory B cells were sorted, how many supernatants were positive, and then how many mAbs were produced? These numbers can be attached to the relevant images in the workflow.*

We modified the figure to include the numbers.

> *(b) For the "Supernatant screening via gamete extract ELISA", please change to "Supernatant screening via gamete/gametocyte extract ELISA".*

We modified the statement as suggested.

> *Line 155: The manuscript states that 84 wells reacted with gamete/gametocyte lysate. The following sentence states that "Out of the 21 supernatants that were positive...". Can the authors provide the summary of data for all 84 wells or why focus on only 21 supernatants?*

We screened all supernatants against gamete lysate, and only a subset against gametocyte lysate. In total, we found 84 positive supernatants that were reactive to at least one of the two lysates. 21 of those 84 positive were screened against both lysates. We have modified the text to clarify the numbers:

“After activation, single cell culture supernatants potentially containing secreted IgGs were screened in a high-throughput 384-well ELISA for their reactivity against a crude Pf gamete lysate (Fig. S1B). A subset of supernatants was also screened against gametocyte lysate (S1C). In total, supernatants from 84 wells reacted with gamete and/or gametocyte lysate proteins, representing 5.6% of the total memory B cells. Of the 21 supernatants that were screened against both gamete and gametocyte lysates, six recognized both, while nine appeared to recognize exclusively gamete proteins, and six exclusively gametocyte proteins.”

Please note that all 84 positive wells were taken forward for B cell sequencing and cloning.

> *Line 171: SIFA is introduced for the first time and should be completely spelled out.*

We have corrected this.

> *Figure 2:*
>
> *(a) In Figure 2A, can you change the column title from "% pos KO GMT" to "% pos Pfs48/45 KO GMT"?*

We have changed the column titles.

> *(b) In Figure 2B, the SMFA results have been converted to %TRA. Can the authors please provide the raw data for the oocyst counts and number of mosquitoes infected in Supplementary Materials?*

We have added oocyst count data in Table S2, to which we refer in the figure legend.

> *(c) For Figure 2F, the authors do have other domains to Pfs230 as described in Inklaar et al, NPJ Vaccines 2023. An ELISA/Western to the other domains could identify the binding site for B2C10L, though we appreciate this is not the central result of this manuscript.*
>
> *We thank the reviewer for this suggestion. We are indeed planning to identify the target domain of B2C10L using the previously described fragments, but agree with the reviewer that this not the focus of the current manuscript and decided to therefore not include it in the current report.*
>
> *Line 116: The word sporozoites appears in subscript and should be corrected to be normal text.*

We have corrected this.

> *Line 216: Typo "B1E11K"*

We have corrected this.

> *Materials and Methods:*
>
> *(a) PBMC sampling: Please add the ethics approval codes in this section.*

Donor A visited the hospital with a clinical malaria infection and provided informed consent for collection of PBMCs. We have modified the method section to clarify this.

“Donor A had lived in Central Africa for approximately 30 years and reported multiple malaria infections during that period. At the time of sampling PBMCs, Donor A had recently returned to the Netherlands and visited the hospital with a clinical malaria infection. After providing informed consent, PBMCs were collected, but gametocyte prevalence and density were not recorded.”

> *(b) Gamete/Gametocyte extract ELISA: Can the authors please provide the concentration of antibodies used for the positive and negative controls (TB31F, 2544, and 399)*

We have added the concentrations for these mAbs in the methods section.

> *Recombinant Pfs48/45 and Pfs230 ELISA: Please state the concentration or molarity used for the coating of recombinant Pfs48/45 and Pfs230CMB.*

We have added the concentrations, i.e. 0.5 µg/mL, to the methods section.

> *Western Blotting: The protocol states that DTT was added to gametocyte extracts (Line 594), but Western Blots in Figures 2 and 3 were performed in non-reducing conditions. Please confirm whether DTT was added or not.*

Thank you for noting this. We did not use DTT for the western blots and have removed this line from the methods section.

> ***Reviewer #3 (Recommendations For The Authors):***
>
> *Below are a few minor comments to help improve the manuscript.*
>
> *(1) In Figure 4E, are the BLI data fit to a 1:1 binding model? The fits seem a bit off, and from ITC and X-ray studies it is known that 2 Fabs bind 1 peptide. The second Fab should presumably have higher affinity than the first Fab since the second Fab will make interactions with both the peptide and the first Fab. It may be better to fit the BLI data to a 2:1 binding model.*

The 2:1 (heterogeneous ligand) model assumes that there are two different independent binding sites. However, the second binding event described is dependent on the first binding event and thus this model also does not accurately reflect the system. Given that there is not an ideal model to fit, we instead are careful about the language used in the main text to describe these results. Additionally, we also include a sentence to the results section to ensure that the proper findings/interpretations are highlighted: "…our data all trend toward the same finding in which a stronger binding affinity is observed toward the longer RESA P2 (16AA) peptide."

> *(2) The sidechain interactions shown in Figures 5C and D could probably be improved. The individual residues are just 'floating' in space, causing them to lack context and orientation.*

We added two panels (Fig. 5C-D) showcasing the binding interface that shows the peptide numbering in the context of the overall complex. We hope that this will help orient the reader.

> *(3) The percentage of Ramachandran outliers should be listed in Table 2. Presumably, the value is 0.2%, but this is omitted in the current table.*

Table 2 has been modified to include the requested information explicitly.

https://doi.org/10.7554/eLife.97865.2.sa0